2010-12-17

Active Noise Control of a Two-Fan Exhaust-Mounted Array Using Near-Field Control Sources and Error Sensors

Ryan Leonard Rust
Brigham Young University - Provo

Active Noise Control of a Two-Fan Exhaust-Mounted Array Using Near-Field Control Sources and Error Sensors

Ryan L. Rust

A thesis submitted to the faculty of
Brigham Young University
in partial fulfillment of the requirements for the degree of

Master of Science

Jonathan D. Blotter, Chair
Scott D. Sommerfeldt
Kent L. Gee

Department of Mechanical Engineering

Brigham Young University

April 2011

ABSTRACT

Active Noise Control of a Two-Fan Exhaust-Mounted Array Using Near-Field Control Sources and Error Sensors

Ryan L. Rust

Department of Mechanical Engineering

Master of Science

Multiple fans are sometimes used in an array configuration to cool various types of electronic equipment. In addition to adding another noise source, using two fans with closely spaced blade passage frequencies (BPF) can create an annoying beat frequency. A two fan array with each fan having a different BPF was considered. The fans were theoretically modeled at the BPF and first harmonics. Each fan has two acoustic paths to the far field. Thus, each fan was modeled as a two source array. The first control configuration consisted of one control filter using six control sources and six error sensors in a fully coupled control system designed to control both fans simultaneously. The second configuration used two independent controllers with three control sources and three error sensors, one controller per fan. Experimentally, the averaged narrow band reduction of the BPFs and the second harmonic of the two independent controllers were 15.6 and 7.4 dB respectively, compared to a reduction of 14.4 and 5.7 dB at the two frequencies using a single control loop. The results suggest that independent controllers perform better than the single control loop for the fan array studied. Optimization of active noise control systems has increased performance but sometimes with decreased robustness. Two control source configurations for the sound power reduction of a simple source were analyzed by modeling the control systems. The two control source configurations were four symmetric control sources surrounding the noise source and an optimized linear array of four control sources. Simulation results show the linear array control source configuration is more sensitive to microphone placement errors, with a 20-33 dB reduction in attenuation for a microphone placement error of 2 mm compared to a 0.8 dB drop in attenuation for the symmetric case. The linear array configuration was found to be more sensitive to the microphone placement errors compared to the symmetric configuration. A 2.5 mm change in one microphone position causes an average of 6 dB loss in attenuation for the linear array configuration compared to a 0.6 dB loss for the symmetric configuration.

Keywords: Ryan Rust, active noise control, sensitivity, axial cooling fan, system modeling

ACKNOWLEDGMENTS

I would like to thank my lovely wife Becky for all her support. I would also like to thank my graduate committee, Dr. Blotter for taking a chance on me, Dr Sommerfedt for introducing me to active noise control and Dr. Gee for letting me build on his work.

TABLE OF CONTENTS

LIST OF TABLES

LIST OF FIGURES

1 INTRODUCTION

1.1 Axial Cooling Fans

1.1.1 Fan Noise

Fans perform a necessary cooling function for many electronics and machines but create noise as a negative byproduct. Figure 1-1 shows the typical spectrum of an axial cooling fan.

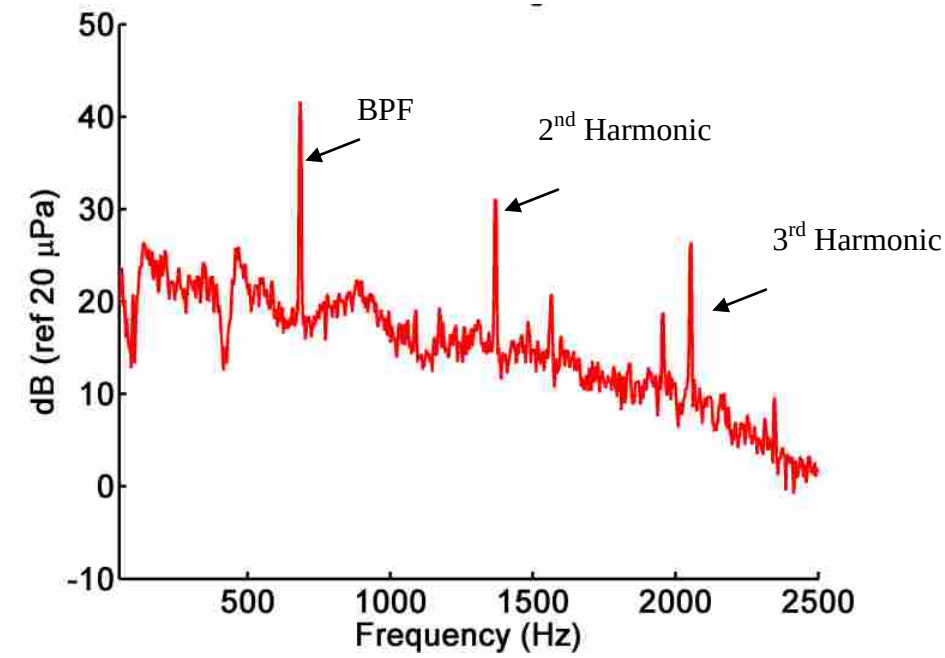

Figure 1-1: Spectrum of a typical axial cooling fan

The fan spectrum shows the largest amplitude tone occurs at around 700 Hz. The noise at this frequency is based on the number of fan blades times the rotation speed of the fan and is

called the blade passage frequency (BPF). Additionally, at multiples of the BPF, there are tonal noise peaks in the spectrum called the harmonics of the BPF, with the 2nd and 3rd harmonics shown in Fig. 1-1. The tonal noise is representative of the "hum" that is associated with a fan in operation. In addition to the tonal noise content, the spectrum also shows broadband noise, which is associated with the "whoosh" sound of the fan.

There are many different noise sources in cooling fans. A study by Huang[1] showed that tonal noise from the axial cooling fans comes from aerodynamic interactions between the fan blades and the stator vanes. Additionally, Huang[1] showed the noise at the BPF acts as an acoustic dipole, which can be represented by two closely spaced acoustic sources of equal magnitude and opposite phase. Additionally, Sharland[2] showed that some of the broadband noise comes from the vortex shedding at the blade trailing edges and from turbulence in the flow. Additional noise sources in the fan result from unsteady loading of the fan or unsteady inlet conditions, turbulent flow through the fan, and trailing edge noise.[1-6] Fitzgerald[7] showed that the tonal noise dominates when the fan has high flow. Modeling and investigating the effective locations of the noise sources in cooling fans has been the subject of many studies, since understanding how the noise is generated by the fan helps engineers implement noise control measures.

Various passive noise control methods have been implemented, but mainly consist of changing the geometry of the fan housing and blades. Shin et al.[8] used response surface methodology to decrease the BPF and the harmonics while maintaining the flow rate and efficiency of the fan. Filleul et, al.[9] changed the inlet to have a bell mouth opening that reduces noise caused by the shroud. Fitzgerald[7] found that fans could be quieted by changing many

aspects of a fan's design including streamlining struts and making parts of the fan more symmetric.

Often times, when a single cooling fan is not adequate to cool a device, multiple cooling fans will be used. Servers, cooling trays, and rack mount electronics are often built to have more than one fan arranged side by side in an array as the cooling solution. These fan arrays often are built with the identical model fan; however, differences in manufacturing cause a slight difference in BPF of each fan, even when the same voltage is applied to the fans. The difference creates a beat frequency that can be annoying. Figure 1-2 shows the narrow band spectrum of two 60 mm fans arrayed side by side.

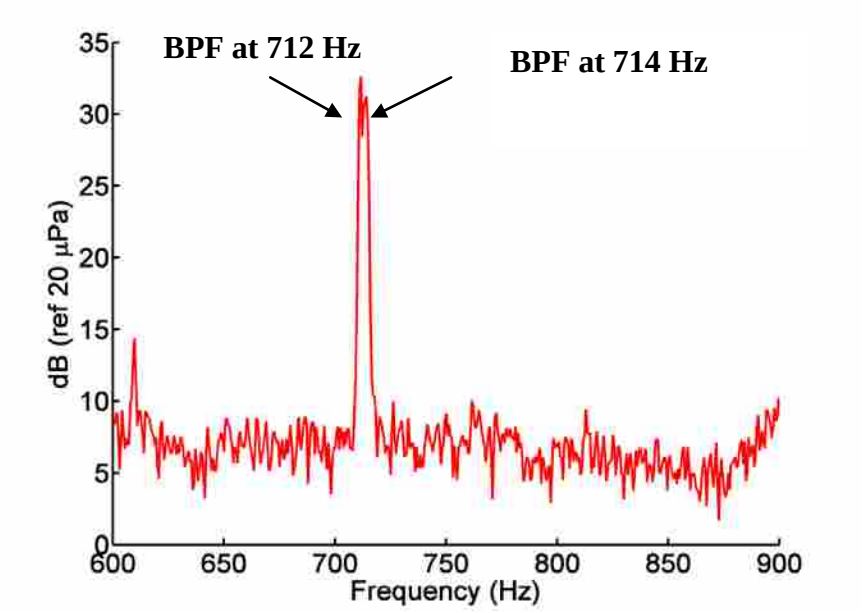

Figure 1-2: Zoom spectrum of the two closely spaced BPFs

In this spectrum, the BPFs of the two fans were separated by 2 Hz in this case, which creates a beat frequency of 2 Hz. A beat frequency results from the superposition of two closely spaced waves that interfere with each other to create low and high amplitude oscillations in the

time signature. The time series of two sinusoids closely spaced in frequency which are added together is shown in Figure 1-3 to demonstrate the beating phenomena.

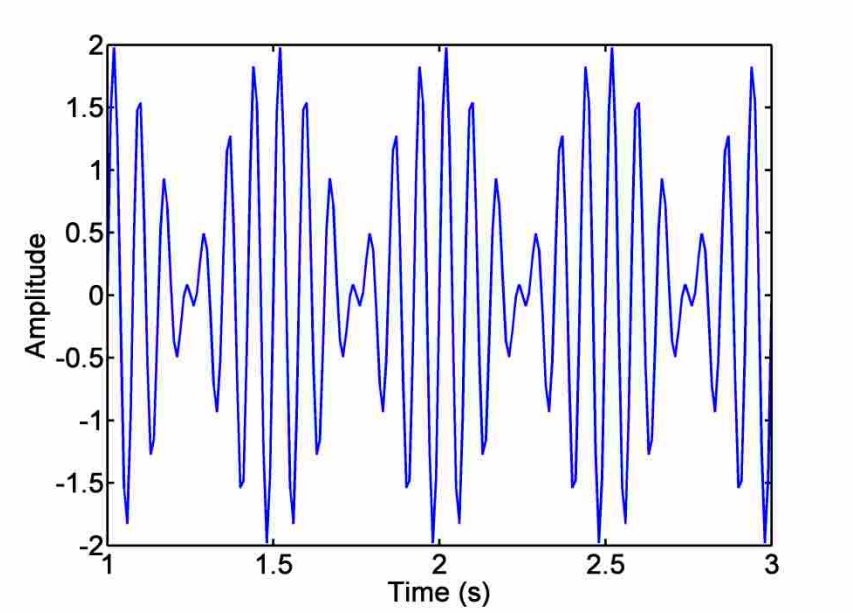

Figure 1-3: The time wave form of two sinusoids with closely spaced frequency showing the beat frequency of 2 Hz.

1.2 **Active Noise Control**

The idea of active noise control (ANC) derives from the superposition of two sound waves of opposite phase and equal magnitude that combine to create zero pressure. Active control gets its name from using speakers to create the canceling wave which adds to the acoustic wave created by the noise source, or in other words from actively adding sound to a noise field. Active noise control was originally proposed by P. Lueg[10], who had the idea patented in 1936. However, it was not until the advent of the digital signal processor that active noise control could be applied to practical applications. Digital signal processors are a key component to many

practical applications of ANC because it provides the computation power to process the real time signals. Recently, the price of digital signal processors has dropped to allow ANC to be a viable option in many noise control applications.

1.2.1 Feed Forward Active Noise Control

Adaptive feed forward ANC is made possible by the development of the filtered-x algorithm, which uses finite impulse response filters to generate the control signal. Feed forward ANC uses knowledge of the impending sound field, called a reference signal, as a basis to create a control signal. The reference signal can be taken from either a mechanical source, such as the signal from an accelerometer or tachometer or an acoustical source, such as the signal from a microphone. The control filter is updated using the least mean square (LMS) algorithm proposed by Widrow et, al.[11-12]

A block diagram of the filtered-x algorithm can be seen in Fig. 1-4. The reference signal, x(t), is a signal that is correlated to the noise, d(t), that is generated by the plant C(z). The reference signal has two roles in the algorithm. First, the reference signal is used with the control filter, W(z), to create the control signal, u(t). The control signal, u(t), then travels through the filters and amplifiers to the control speaker and propagates to the error sensor. This total transfer function is called the secondary path, H(z), and the output of this secondary path, y(t), is measured at the error microphone. The principle of superposition says that pressures add at the error microphone or some other acoustic sensor. Thus, the output of the controller plus the disturbance noise gives the error, e(t). The second use of the reference signal is to update the control filter. The reference signal is first filtered by an estimate of the secondary path H'(z) creating the filtered-x signal, r(t). The reference signal is first filtered to increase the stability of

the control system. The error signal and filtered-x signals are now used in the LMS update to adaptively change the control filter.

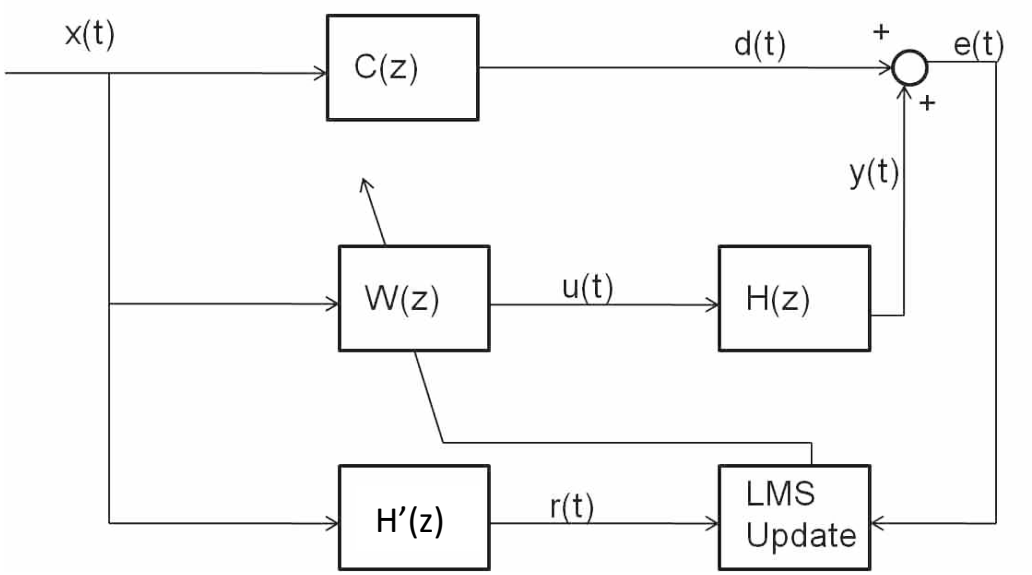

Figure 1-4: The Filtered-x algorithm

The LMS update is derived from the squared error and uses a steepest descent gradient to update the control filter. The convergence parameter, μ, must be large enough to track changes in the noise, but also small enough to maintain stability. Filtered-x update equation then becomes

$$W(n+1) = W(n) - \mu e(t) R(t) \qquad (1\text{-}1)$$

The update equation means that the next control filter is taken from the old control filter minus the gradient, were R(t) is a vector of the last N values of r(t) and where N is the length of the control filter. Feed forward active noise control is often used for tonal noise sources of revolving equipment like engines and fans.

1.2.2 Free Field Active Noise Control

Implementation of ANC minimizes the squared pressure or other acoustic signal at an error sensor. In ANC, when the noise at the error sensors is driven to zero by the control system, the result is not always a reduction in the overall sound power. The placement of the error sensors and control sources impact the reductions achieved by the control system. Source coupling is a way to globally reduce the noise. The concept of source coupling is demonstrated by a dipole source configuration which consists of two closely spaced simple sources of the same magnitude and opposite phase. Figure 1-5 shows the relative sound power of a two simple sources of equal phase and opposite magnitude to a monopole source based on the kd of the dipole, where k is the wave number and d is the distance between the two sources and kd is a measure of distance relative to the acoustic wavelength. The figure shows that as the two sources are brought closer together relative to wavelength, they create a dipole, i.e., a small kd, the sound power relative to monopole goes to zero.

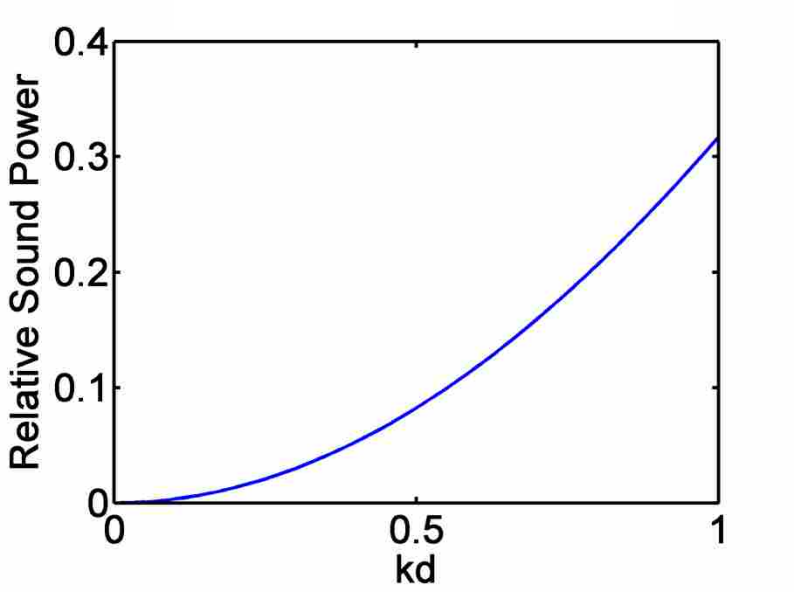

Figure 1-5: The relative power of a dipole compared to a monopole as a function of kd

Applying the dipole source coupling idea, Nelson et, al.[14-15] minimized the sound power by introducing closely spaced control sources relative to a wavelength. The closely spaced control sources modify impedance for the primary source, basically inhibiting the primary source from radiating noise. All acoustic sources create impedances between themselves and the other acoustic sources, including self impedance. Nelson et al.[14-15] showed that the complex impedance between two simple sources is given by

$$Z(kd) = \frac{jk^2\rho_o c}{4\pi}\left(\frac{e^{-jkd}}{kd}\right), \tag{1-2}$$

where k is the wave number, d is the distance between the two sources, ρ_o and c are the density and speed of sound in the medium respectively. An impedance matrix, $\overline{\boldsymbol{Z}}$, can be constructed whose elements consist of the impedance between all the sources in a system, including the self impedance, with each term obtained from using Eqn. 1-2. Using this impedance matrix, the total sound power radiated from a system of sources can be represented by,

$$\Pi = \frac{1}{2}\bar{\mathbf{Q}}^{H}\mathrm{Re}[\bar{\mathbf{Z}}]\bar{\mathbf{Q}} \tag{1-3}$$

where $\bar{Q}$ is the vector of complex source strengths for all sources in the system. Breaking this power equation into primary source and control sources, the total sound power can be rewritten as

$$\Pi = \bar{\mathbf{Q}}_c^{H}\bar{\mathbf{A}}\bar{\mathbf{Q}}_c + \bar{\mathbf{B}}^{H}\bar{\mathbf{Q}}_c + \bar{\mathbf{Q}}_c^{H}\bar{\mathbf{B}} + C \tag{1-4}$$

where

$$\overline{\boldsymbol{A}} = \frac{1}{2}\mathrm{Re}\left[\overline{\mathbf{Z}}_{cc}\right], \tag{1-5}$$

$$\overline{\boldsymbol{B}} = \frac{1}{2}\mathrm{Re}\left[\overline{\mathbf{Z}}_{pc}\right]\overline{\mathbf{Q}}_p, \tag{1-6}$$

$$C = \frac{1}{2}\overline{\mathbf{Q}}_p^{H}\mathrm{Re}\left[\overline{\mathbf{Z}}_{pp}\right]\overline{\mathbf{Q}}_p, \tag{1-7}$$

with $\overline{\boldsymbol{Z}}_{cc}$ being an impedance matrix between each control source and all other control sources, $\overline{\boldsymbol{Z}}_{pc}$ is the impedance matrix between control sources and the primary sources, $\overline{\boldsymbol{Z}}_{pp}$ is the impedance matrix between all the primary sources, $\overline{\boldsymbol{Q}}_{p}$ is a vector of the complex source strengths of the primary sources and $\overline{\mathbf{Q}}_{\mathrm{c}}$ is a vector of the complex source strength of the control sources. Taking the derivative of Equation 1-4 with respect the control source strength vector and setting the result equal to zero results in the source strength vector that minimizes the sound power:

$$\overline{\mathbf{Q}}_{\mathrm{so}} = -\overline{\mathbf{A}}^{-1}\overline{\mathbf{B}} \tag{1-8}$$

Substituting this source strength into the sound power equation results in the minimum sound power of the configuration of sources given by

$$\Pi_{\mathrm{min}} = \mathrm{C} - \overline{\mathbf{B}}^{\mathrm{H}}\overline{\mathbf{A}}^{-1}\overline{\mathbf{B}}. \tag{1-9}$$

The minimized sound power can now be divided by the sound power of the primary sources to find the attenuation of the primary source.

Many factors go into implementing this type of control system as set forth by Synder[16], who developed a pyramid of important control system factors as shown in Fig. 1-6. The pyramid is arranged so that the bottom part is the most important design aspect in achieving attenuation and progressively gets less important going to the top of the pyramid.

In the sound minimization technique, the arrangement of the control sources becomes the greatest factor in maximizing attenuation of the primary source.

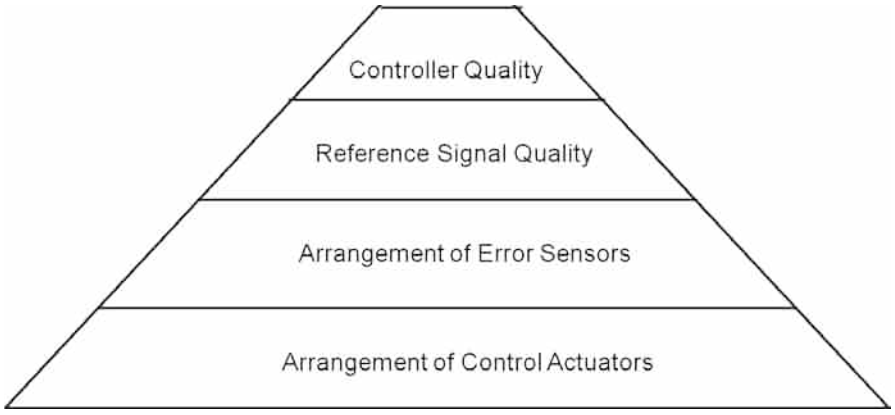

Figure 1-6: Global control hierarchy with the bottom the most important factor[16]

An additional aspect that needs to be considered in setting up this type of control is the position of the error sensors. The right configuration of control sources will not automatically converge to the optimal source strengths to minimize sound power. The error microphones must be placed in the right locations to force the controller to the optimal source strengths. As with any feed forward active noise control system, the reference signal has to be correlated with the noise in order for the noise source to be attenuated. The control algorithm must be able to drive the error to zero without going unstable.

1.2.3 Implementation of Active Control on Cooling Fans

Passive noise control efforts have been successful but the methods have limitations. Hence, active noise control of axial cooling fans has been the subject of many studies.[17-28] Since many control configurations have been studied a only a few will be outlined here. A simple control system implemented by Quinlan[18] used a single source located next to the fan demonstrating that active noise control could be applied to a cooling fan. Also, Wang[19] used an uncapped speaker acting as a dipole and combined with the dipole nature of a fan to create a lateral quadrupole to reduce noise emission from the fan. More complex control configurations

have since been attempted. Wang et al.[20] used a four speaker array of speakers to control the drag noise of the fan. Two of the speakers were on top of the fan, with one speaker being placed pointing away from the fan, and the other facing the same direction as the fan. The two remaining speakers were placed on the bottom of the fan in the same type of speaker configuration. Lauche[21] used the fan itself as the control source, creating a small distance between the control source and the primary source. A shaker was used to make the fan into a control source to attenuation noise radiated from the fan.

Notably, Gee and Sommerfeldt[22-23] surrounded the fan with four control sources in a symmetric control configuration, but also created a compact system by placing the error sensors in the near-field. Applying the sound minimization technique to cooling fans, Gee and Sommerfeldt found the optimal near-field error microphone locations by a) modeling all sources as monopoles, b) using the Nelson et al.[14-15] method to minimize the radiated power, and c) finding where the calculated near-field pressure level reduction was the greatest. However, because minimization of squared-pressure at discrete locations does not necessarily guarantee the source coupling that will result in minimized radiated power, near-field measurements were used to confirm the validity of this approach.[24]

Few efforts have been made to actively control multiple cooling fans. There are two US patents that explain ways to control the noise and beat frequency of fan arrays. Abali et al.[25] have reduced noise at the blade passage frequency of a fan array by using the other fans in the array as control sources. The speed of the control fan is changed to minimize the radiated sound. Lyszkowski and Wallace[26] control the beating by changing the speed of the fans to match each other.

1.2.4 Optimization of Control Source Locations

Optimization of error sensor and control source placement has also been the subject of many active control studies.[27-34] For instance, Clark and Fuller[27] used an algorithm to optimize the placement of a piezoelectric actuator and strain error sensor to control the sound from a baffled simply supported plate. Berkhoff[28] found that there is an optimal distance between control sources and error sensors which is related to the distance between the control sources for the active control of sound transmission through a plate. Pulthasthan and Pota[29] used an energy-based approach to find the optimal actuator and sensor locations to control structural radiation. Additionally, genetic algorithms have also been implemented to find the optimal locations for control sources and error sensors.

Specifically, Duke et al.[30] used a genetic algorithm to improve upon the control source arrangement used by Gee and Sommerfeldt for an axial cooling fan. The results showed that including the primary source within a linear array of control sources resulted in the source configuration that minimized the radiated power. Experiments showed improved performance relative to Gee and Sommerfeldt's symmetric source arrangement. Figure 1-7 shows the experimental results from the linear array verses the surrounding configuration used by Gee.

The theoretical results predict large improvements of the control system for the linear array configuration. However, when controlling a speaker, experimental results were unable to match the theoretical results. The linear array configuration predicted a reduction of 58.4, 33.4 and 17.7 dB of the sound power at 550, 1100 and 1650 Hz respectively but experimental results only achieved 32.4, 23.2 and 3.0 dB.

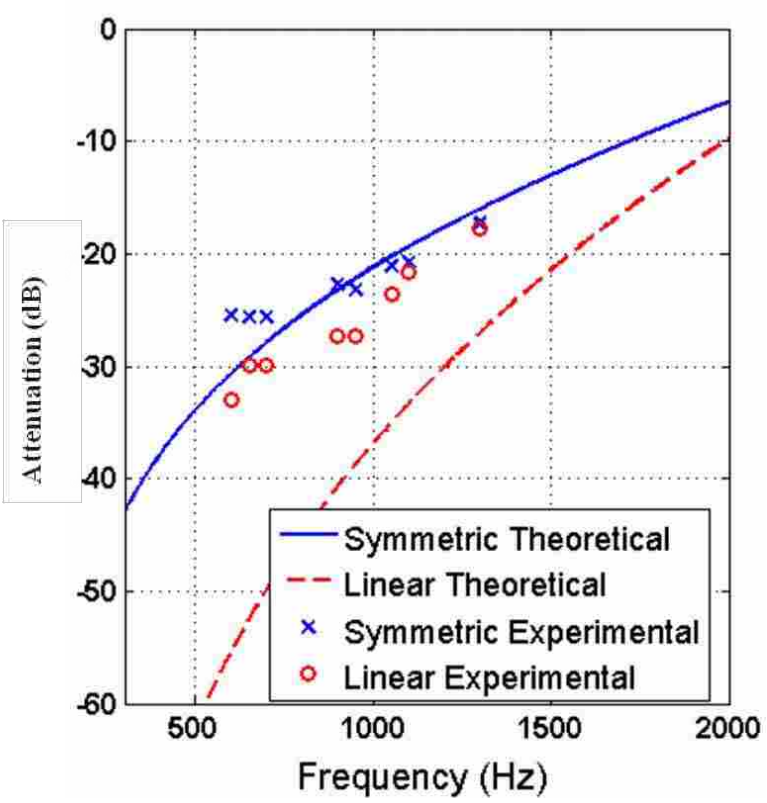

Figure 1-7: Experimental results for the sound power attenuation of the primary source for the linear array and symmetric control configuration.[30]

1.3 **Objective**

Two main objectives will be considered for this thesis. The first objective is to study active noise control of a closely spaced two fan array with the two fans having slightly different BPFs. Two different control strategies will be implemented to the two fan array system. First, a single control system that controls the BPFs and first harmonics of both fans. Second, two independent controllers implemented to control each fan individually, comparing these two results will show whether each fan in the array can be modeled and controlled individually as independent sources.

The second objective is to investigate how control source configurations affect the robust nature of a control system. Since the linear array of control sources was unable to achieve the theoretical results, a sensitivity analysis of the linear array of control sources verses a symmetric configuration is performed. The control system is modeled as four baffled point sources. The squared pressure at four locations will be driven to zero representing the four error microphones. The purpose of the simulation is to analyze the effect of sensor placement error and the sensitivity of the control system to extraneous noise sources on the two control source configurations. Additionally, the simulation will provide insight into the reasons why the linear configuration of control sources does not achieve the predicted attenuations.

1.4 **Thesis Outline**

The next two chapters present papers that will be submitted for publication. Chapter 2 presents a paper on the active control of multiple cooling fans covering the study into the first objective of the thesis. The paper shows the modeling and experimental work of actively controlling a two fan array. Building upon the optimization set forth by Duke, et al.[30] Chapter 3 presents an analysis of two control configurations for a single axial cooling fan. The analysis was performed using a simulation tool to test the sensitivity of the two control configurations to error sensor placement and noise sources. The chapter includes simulations of a control system as well as the experimental confirmation of the results and contributes to objective two of the thesis. Chapter 4 has the conclusions and recommendations for possible future work.

2 ACTIVE NOISE CONTROL OF A TWO-FAN EXHAUST-MOUNTED ARRAY USING NEAR-FIELD CONTROL SOURCES AND ERROR SENSORS

2.1 Abstract

Multiple fans are sometimes used in an array configuration to cool various types of electronic equipment. In addition to adding another noise source, using two fans with closely spaced blade passage frequencies (BPF) can create an annoying beat frequency. In this work, a two-fan, exhaust-mounted array was considered for active noise control of the BPF and 2nd harmonic of each fan. In this array, each fan has a different BPF, as such, the fans were theoretically modeled individually at the 4 frequencies of interest. Each fan has two acoustic paths to the far field. First the direct radiation and a second acoustic path from the back of the fan through the box and out the other fan opening, creating a second virtual source at the location of the other fan. Therefore, in this work, each fan was modeled as a two source array because of the two acoustic paths. Two control configurations were theoretically and experimentally compared. The first control configuration consisted of one control filter using six control sources and six error sensors in a fully coupled control system designed to control both fans simultaneously. The second configuration used two independent controllers with three control sources and three error sensors, one controller per fan. Theoretically, at 712 Hz the nominal BPF of the fans in the array, the second acoustic path greatly affects the theoretical attenuation of the 3 control source implementation dropping the attenuation from 23 dB to 7 dB in extreme cases, but barely impacts the 6 control source implementation. If the second acoustic path was negligible, the 6 control source configuration only has 3 dB more sound power attenuation of the

BPFs than the two 3 control source implementation. The 6 source control configuration requires microphone positions which were optimal for both fans. The shared microphones in this configuration cause limited optimal placement compared to the individual controllers. Experimentally, the averaged narrow band reduction of the BPFs and the second harmonic of the two independent controllers were 15.6 and 7.4 dB respectively, compared to a reduction of 14.4 and 5.7 dB at the two frequencies using a single control loop. The results suggest that independent controllers perform better than the single control loop for the fan array studied. The limited optimal error sensor placement of the error microphones impacted the performance of the 6 control source implementation. Additionally, the independent controllers required less computation time because this implementation used less finite impulse response filters than the 6 control source configuration. The active noise control of the BPFs caused the amplitude of the tonal components in the beat frequency to be low, making the beating less noticeable.

2.2 **Introduction**

Arrays of cooling fans are often used in applications such as servers and cooling trays. Compared to a single fan, multiple fans improve cooling but also increase noise levels by adding a second noise source. Huang[1] showed the tonal noise from axial cooling fans comes from aerodynamic interactions between the fan blades and the stator vanes. The frequency of the lowest tone, which is called the blade passage frequency (BPF), is found by the number of fan blades multiplied by the rotation speed. Huang[1] also showed that the radiation at the BPF acted like a dipole noise source. Additional tones at the harmonics of the BPF are also present in the noise spectrum. Broadband noise from cooling fan comes from various sources, including the vortex shedding at the blade trailing edges and from turbulence in the flow.[2-3]

When using two or more cooling fans, manufacturing differences cause identical model fans to generally rotate at slightly different speeds, even when the same voltage is applied. When the BPFs are sufficiently close together, they create an audible beat frequency. Means of eliminating the beat frequency have been explored by various researchers; including synchronizing the speed of one fan to match the speed of the other.[25] Another proposed method is for one fan to be the control source to actively control the noise of the other fan.[26]

The active control of the tonal noise content from axial cooling fans has been studied using various control configurations. Control source configurations have ranged from a single control source to multiple control sources surrounding the fan.[18-24] Gee and Sommerfeldt[22-23] used a sound power reduction technique proposed by Nelson *et al*.[14] In this technique, the sound power of a simple source can be minimized by introducing control sources that are closely spaced to the primary source, relative to an acoustic wavelength.

Gee and Sommerfeldt[22-23] surrounded the baffled fan with four symmetrically placed control sources. Modeling the control sources and fan as simple sources, they determined the optimal control source strengths to minimize the sound power. Using these source strengths, the near-field controlled pressure field relative to the primary pressure field was determined. Near-field control microphones were then placed at locations of maximum attenuation in the relative pressure field. With the error microphones placed in these locations, the BPF and harmonics were controlled globally for an axial cooling fan.

The purpose of this paper is to extend the approach implemented by Gee and Sommerfeldt[22-23] and later by Monson *et al*.[35] and Shafer *et al*.[24] from a single exhaust-mounted cooling fan to an exhaust-mounted, two-fan array. Fan arrays pose additional problems beyond a single fan system. The proximity of the two fans affects the control source configuration that

can be implemented. Gee and Sommerfeldt[22-23] used four symmetrically and closely spaced control sources surrounding the fan which cannot be used for this two-fan array. Having two fans in the array creates two acoustic paths for the noise to travel. First, direct path radiation and second noise from the back side of each fan through the box and out of the other fan opening, creating a virtual noise source at the location of the other fan. The two acoustic paths effectively turn each fan into a two source array.

In implementing the active noise control, two different control configurations were considered. First, two independent controllers were used to control the two fans independent of the other fan. Second, a single control loop was used to actively control both fans, using a fully coupled control system that surrounds the fan array. Theoretically, the sound power attenuations of a two primary source array using both of these control configurations were determined. The optimal control source strengths were used to create the near-field controlled pressure relative to the primary field to find microphone placement locations. Using the two control configurations and the theoretical error sensor placement locations, active noise control was applied to a two fan array.

2.3 **Theoretical Development**

A two fan array with the fans arranged side by side was considered for this paper. Following the same procedure as Gee and Sommerfeldt,[22-23] each fan in the array was modeled as an independent simple noise source because each fan generally had a different BPF. Huang[1] showed that the BPF of a single fan radiates as a dipole. As such, there was noise radiated from both the front and back of the fan. Noise from the back side of the fan radiates through the box and out the other fan opening. The second acoustic path creates a virtual noise source at the

location of the other fan. Therefore, each fan in the array was modeled as two closely spaced simple sources.

Gee and Sommerfeldt[22-23] placed four equally-spaced control sources surrounding the fan with one source on each side of the square surrounding the fan. However, here the two fans were placed side by side close together, not allowing the fourth control source to surround each fan. The control sources were instead placed surrounding fan array. The modeled control of a single fan in the array surrounded by 6 control sources is shown in Fig. 2-1.

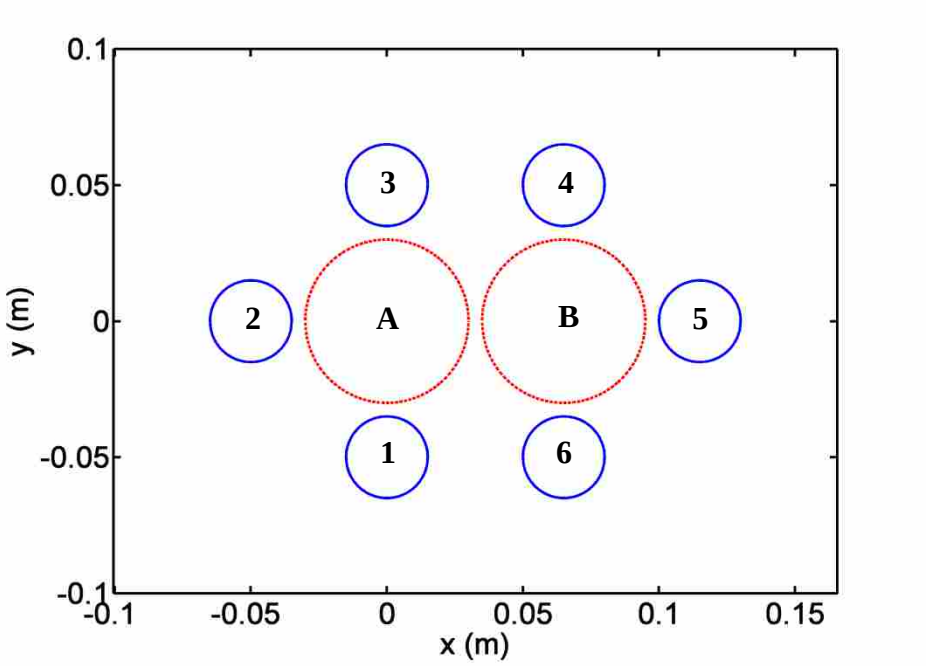

Figure 2-1: The location of the primary and control sources with the primary sources being red dashed circles and the control sources blue solid circles

Primary source A in Fig. 2-1 is representative of the main acoustic path of the fan from the front side of the fan. Primary source B is a flanking source representative of the acoustic path from the back side of the fan through the box and out the other fan hole. Two control source configurations were investigated to control these two closely spaced primary sources. The first

control configuration used control sources 1-3. The second control implementation used all six control sources shown in Fig. 2-1. The BPFs of the two fans were determined to be 712 and 714 Hz, so 712 Hz was used in the theoretical analysis. The phase and magnitude of primary source B relative to A was unknown for the experimental array. The sound power attenuation of various primary source arrays was determined to find the potential impact of source B on the two control configurations. The sound power attenuation (in dB) is shown for various primary source arrays in Table 2-1 with the relative phase and magnitude of source B compared to source A.

Table 2-1: Sound power attenuation of a two primary source array of a three and six control source configuration, shown are the magnitude and phase of primary source B relative to primary source B.

Relative Magnitude	*Relative Phase*	*Attenuation (dB)*	
		3 Sources	6 Sources
1	0	16.0	26.9
1	90	14.6	27.1
1	180	7.1	34.2
0.5	0	18.1	26.9
0.5	90	18.0	27.1
0.5	180	17.0	28.4
0.25	0	20.2	27.0
0.25	90	21.3	27.1
0.25	180	26.2	27.5
0	0	24.2	27.1

Table 2-1 shows that the 6 control source configuration is robust and is relatively unaffected by different possible primary source arrays. The theoretical attenuation does not drop below 26.6 dB across all the possible primary source arrays for this control configuration. Looking at the three control source configuration results, if primary source B is significant compared to source A then the configuration is greatly impacted dropping to 7 dB in the worst case. However, as the magnitude of the second primary source drops, the difference between the two control source configurations was lessened until there was only a 3 dB difference between the two control

implementations when the source B is neglected. Depending on the magnitude and phase of the acoustic path from the back side of the fan, there is a large impact on which control configuration would be optimal to use on the fan array.

The theoretical microphone positions were found in the same manner as Gee and Sommerfeldt.[22-23] The optimal control source strengths were used to minimize the sound power to predict near-field controlled pressure relative to the primary source pressure field. The places of maximum attenuation of the primary field correspond to optimal error microphone locations.

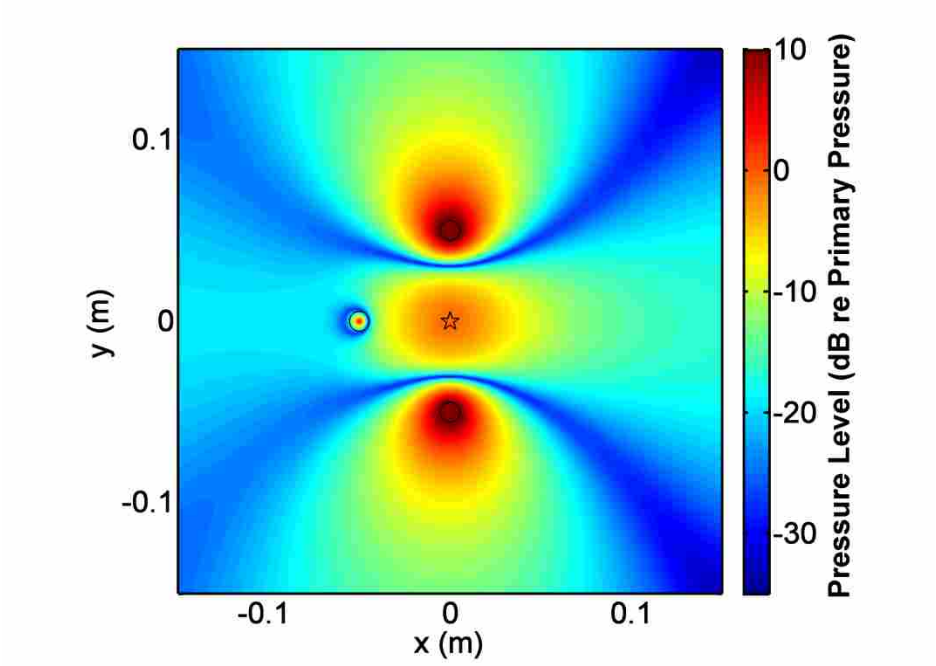

Figure 2-2: The near-field pressure of the controlled field relative to the primary field, in dB, for a three control source and one primary source configuration. The nulls in the near field are the ideal locations for the error sensors, the circles show the locations of the control sources and the star is the primary source location.

The primary source array is unknown, so the most simplistic case of primary source B with zero magnitude will be used to demonstrate how the microphone placement in the control

system is determined. In this case, the controlled near-field pressure relative to the primary field is shown in Fig. 2-2 for the three control source configuration.

The places of maximum attenuation in the pressure map shown in Fig. 2-2 represent the optimal locations for the error sensors in the near field to obtain maximum sound power attenuation of the primary source. In this case, the control system should converge to having control source 2 (on the left side) go toward zero, leaving two control sources effectively controlling the primary source.

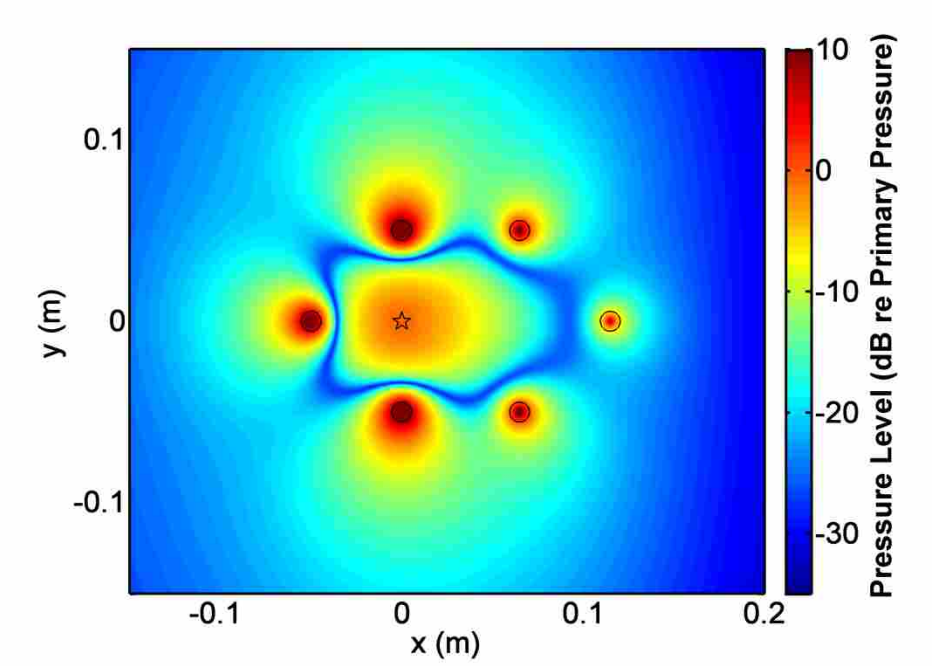

Figure 2-3: The near-field pressure of the controlled field relative to the primary field, in dB, for a six control source and one primary source configuration. The nulls in the near field are the ideal locations for the error sensors, the circles show the locations of the control sources and the star is the primary source location.

For the three control source configuration each fan had an independent controller. Thus, for the second fan in the array the same plot (mirrored about the y-axis) would be used for the

second fan at the frequency of interest. The relative near field pressure map for the six control source configuration is shown in Fig. 2-3, again for the case of having only one primary source. The error microphones should be located along the pressure minima in Fig. 2-3. When applying the six control source configuration to a fan array, both fans were controlled with shared error microphones. Therefore, the error microphones need to be in optimal locations for each fan. A similar pressure map can be made for the second fan in the array. The two pressure maps can be overlapped with the optimal error sensor locations were found by the intersection of the pressure minima of the two maps, the intersection map is shown in Fig. 2-4.

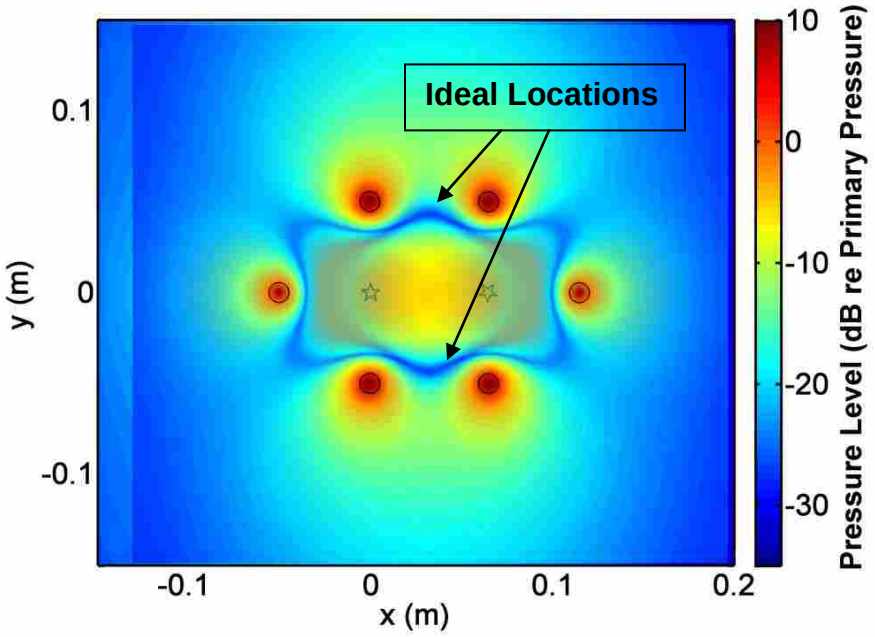

Figure 2-4 : The overlapped near-field pressure of the controlled field relative to the primary field, in dB, for a six control source and one primary source configuration for each fan in a two fan array. The cross section of the nulls in the near field are the ideal locations for the error sensors, the circles show the locations of the control sources and the stars the locations of primary sources.

Looking at Fig. 2-4, the optimal placement for both fans was limited to in between the two primary sources. The limited error sensor placement locations means that in practice the control system might not be able to achieve the theoretical sound power reductions because optimal microphone placement locations might not be available for both fans.

In the experimental set up used to test the active noise control on the fan array, the magnitude of the primary source B comparative to source A was unknown; therefore, the ideal microphone placements were also unknown. An estimate of primary source B relative to source A was determined for a fan in the experimental array.

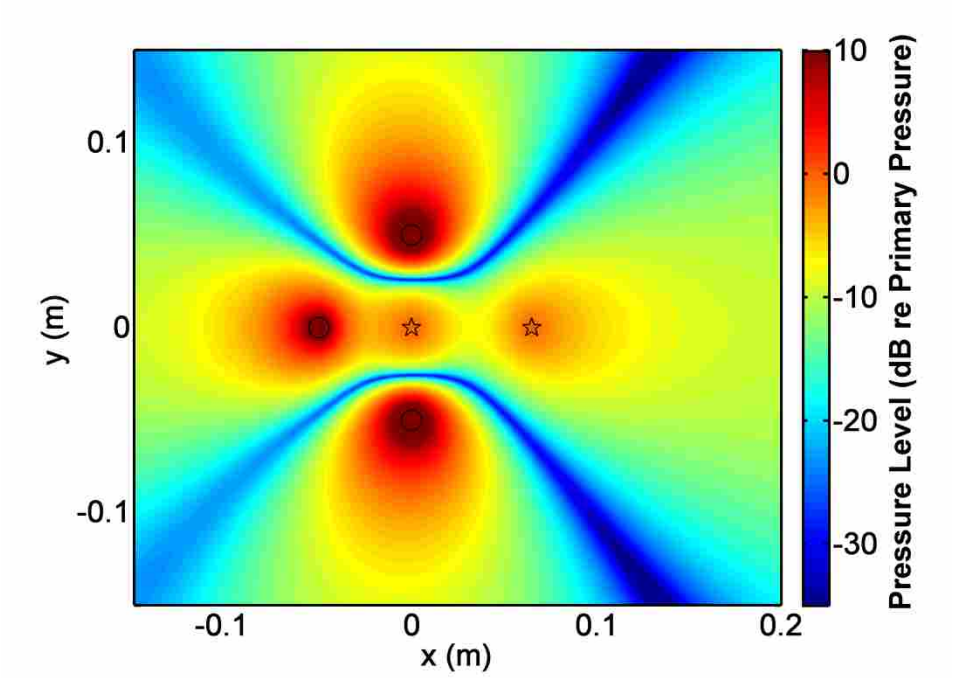

Figure 2-5: The overlapped near-field pressure of the controlled field relative to the primary field, in dB, for a three control source and two primary source configuration. The nulls in the near field are the ideal locations for the error sensors, the circles show the locations of the control sources and the stars are the primary source locations.

A baffle was placed in between the two fans, isolating the two primary sources. A microphone was placed on each side of the baffle just outside each fan opening. With one fan in

operation, the transfer function between the two microphones was used to estimate the magnitude difference at the BPF between the two acoustic paths. The magnitude difference was estimated to be 7 dB. Looking at Table 2-1, the estimated magnitude ratio of 0.44 between the primary and secondary path means that the 6 control source configuration would theoretically have approximately 10 dB more attenuation than the 3 control source configuration.

Using the magnitude data, the error sensor placement can be approximated with creating new pressure maps. The near field control pressure field relative to the primary field for the 3 control source configuration is shown in Fig. 2-5 with a second primary source B with a relative magnitude of 0.44 and no phase difference to primary source A. The places of maximum attenuation in the plot were used as the microphone placement for the two fan array tested in this paper.

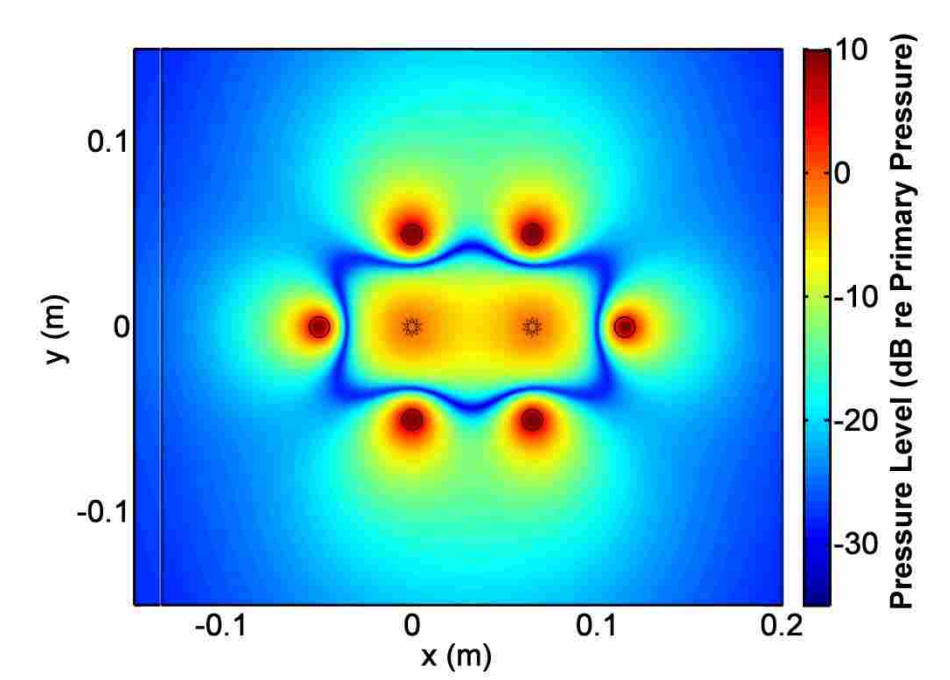

Figure 2-6: The overlapped near-field pressure of the controlled field relative to the primary field, in dB, for a six control source and two primary sources configuration. The cross section of the nulls in the near field are the ideal locations for the error sensors, the circles show the locations of the control sources and the stars the locations of primary sources.

Similarly, the overlapped relative control pressure field to the primary field for the 6 control source configuration is shown in Fig. 2-6. The optimal microphones locations in this theoretical plot were used in the experimental active noise control on the two fan array. The maximum sound power attenuation for the 3 control source configuration at the BPF is 16-17 dB and 27 dB for the 6 control source configuration.

2.4 **Experimental Setup**

An exhaust-mounted two fan array was constructed with two identical 60 mm axial cooling fans. The fan array was in a computer sized box with dimensions of 46 x 42 x 22 cm. The two fans were spaced 6.5 cm apart, center to center. The control sources were 2.5 cm HiVi and were placed according to Fig. 2-1 with the complete set up is shown in Fig. 2-7

Feed-Forward active noise control requires a reference signal that is correlated to the noise and the fans used did not have a built in tachometer like many fans. Therefore, the reference signal was taken from an emitter detector pair mounted on the fan that gives a pulse each time a fan blade passes. This method has been used in a number of previous studies.[22-23,24,35]

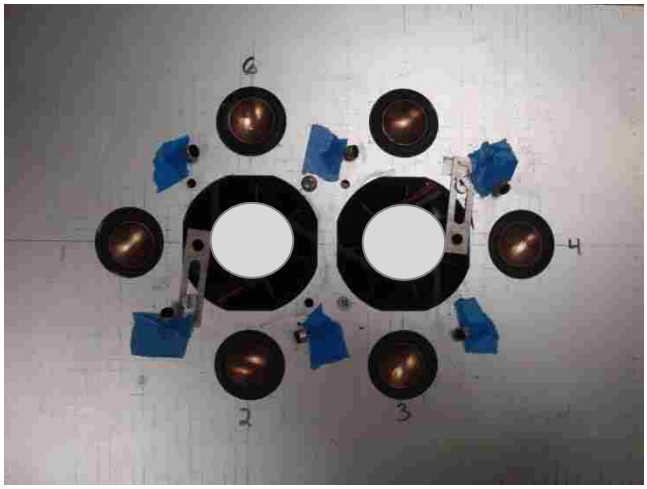

Figure 2-7: The control setup used for the active control of a two fan array

For the six control source configuration, the reference signals from each fan were mixed and used in the single control loop. The control filter utilized 128 coefficients and 20 coefficients were used for the secondary path model. When implementing the two control filter loop with three control speakers and three error microphones for each loop, one of the fan reference signals was used in each control loop, with 20 control filter coefficients and 20 secondary path model coefficients in each loop. The error microphones were 6mm Hosiden electret microphones. The error sensors were placed on the theoretical pressure minimum locations found previously. Anti-aliasing low-pass filters were implemented with a cutoff frequency of 1800 Hz using 8 pole Krohn-Hite 3384 filters. The DSP board was based on a Texas Instruments 320c6713 chip and used a 4000 Hz sampling frequency.

The fan array was placed in an anechoic chamber to measure the sound power reduction at the tonal frequencies. A characteristic measurement was an on-axis measurement of the fan noise spectrum with 0.6 Hz resolution to find the beat frequency of the fan array at 1.7 m using a GRAS 12.7 mm type I microphone. The sound power measurement of the fan array was obtained

using a semicircular array with a radius of 1.7 m and 13 GRAS 12.7 mm type I microphones equally placed along the semicircle and can be seen in Fig. 2-8.

The fan array was placed under the center microphone of the semicircular array, and the measurement array was rotated about the center microphone at 15 degree increments to create a 360 degree scan. At each microphone position, the autospectrum was calculated using 15 averages and a frequency resolution of 6.1 Hz. The sound power was calculated using the autospectrum with a method used by Monson et al.[10] who used an area weighting function to determine the sound power.

Figure 2-8: Picture of the 13 microphone measurement array in the anechoic chamber

The measurement was repeated 5 times with and without active noise control. The resulting sound powers were then averaged to find the performance of the single control loop and for two control loops.

2.5 **Results and Discussion**

The characteristic noise spectrum of this two fan array is shown in Fig. 2-9. The figure shows the frequencies that were targeted by the control system, consisting of the BPFs and 2nd harmonics at 712, 714, 1424 and 1428 Hz, respectively. Highlighting the beating of the fan, Fig. 2-10 shows a zoom spectrum of the BPFs. The BPF peaks are 2 Hz apart, creating an audible beat frequency.

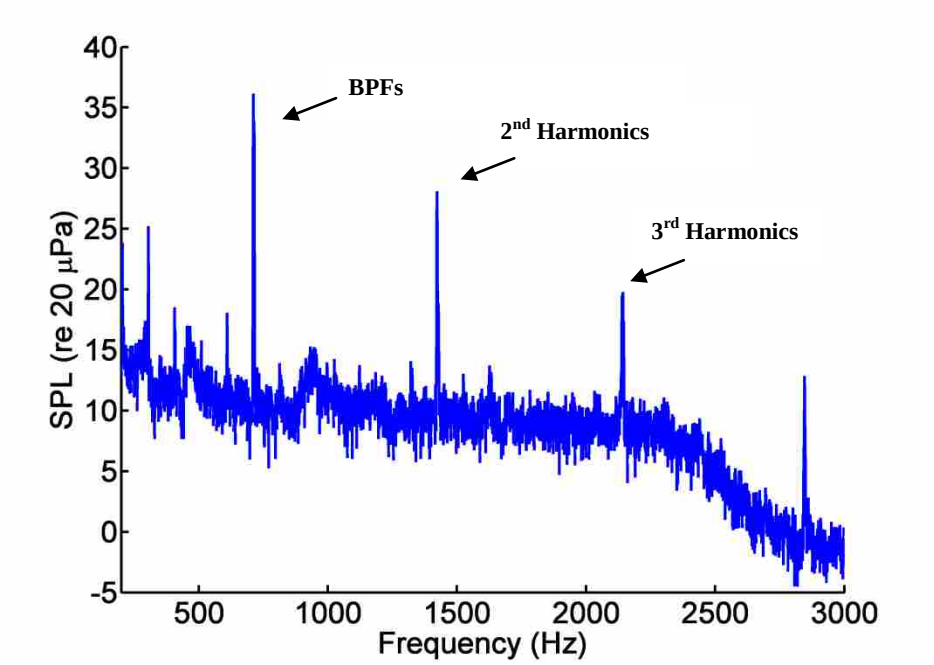

Figure 2-9: Noise spectrum of a two fan array measured 1.7 m on axis with the array.

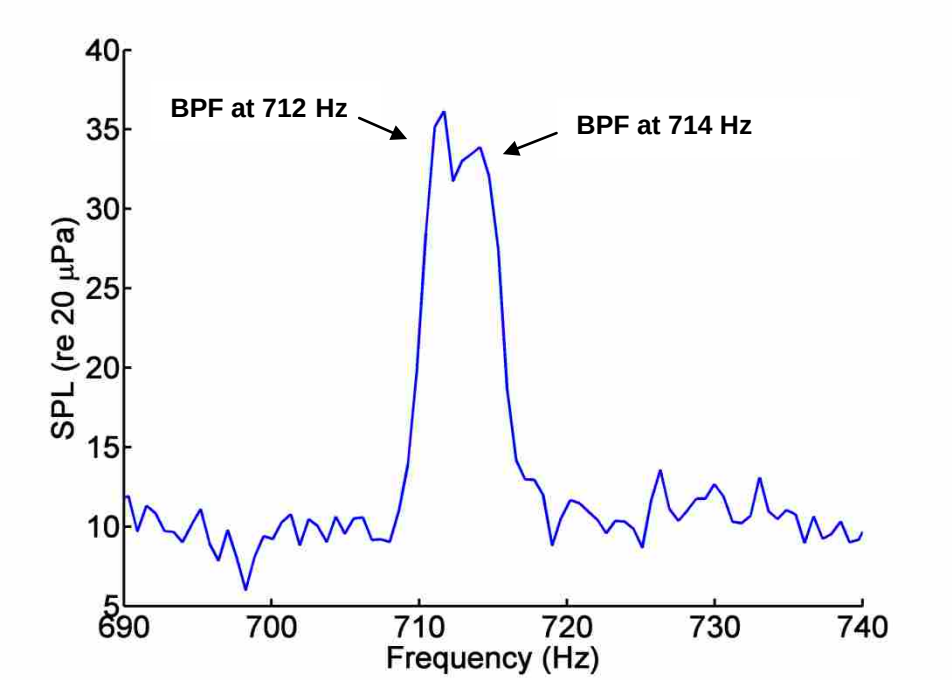

Figure 2-10: The noise spectrum measured 1.7 m away from the center of the fan array, showing the two BPFs 2 Hz apart.

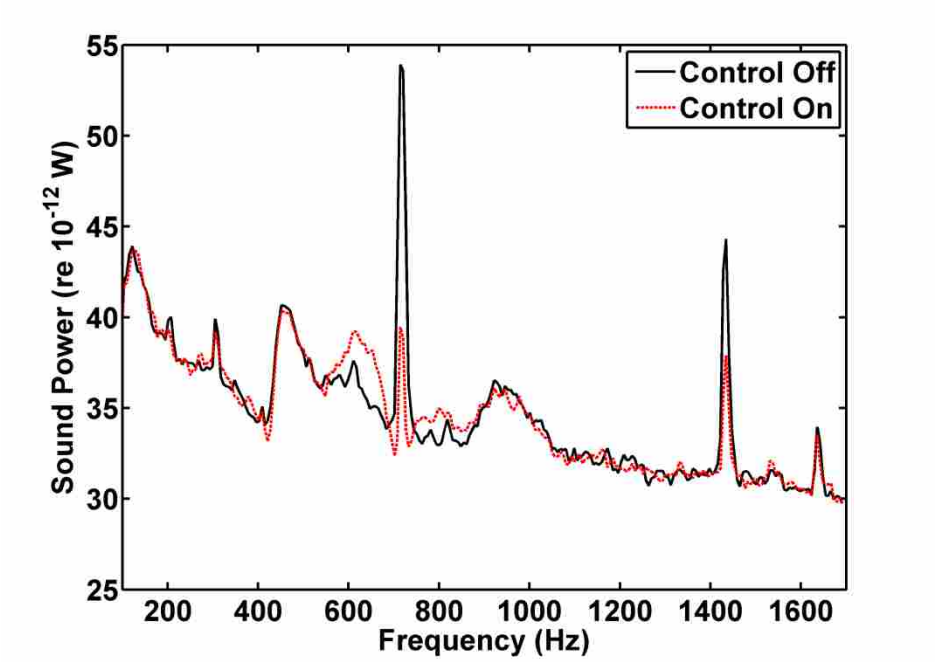

Figure 2-11: Sound power with control on and off of a two fan array using a single six control source by 6 error sensor controller for both fans.

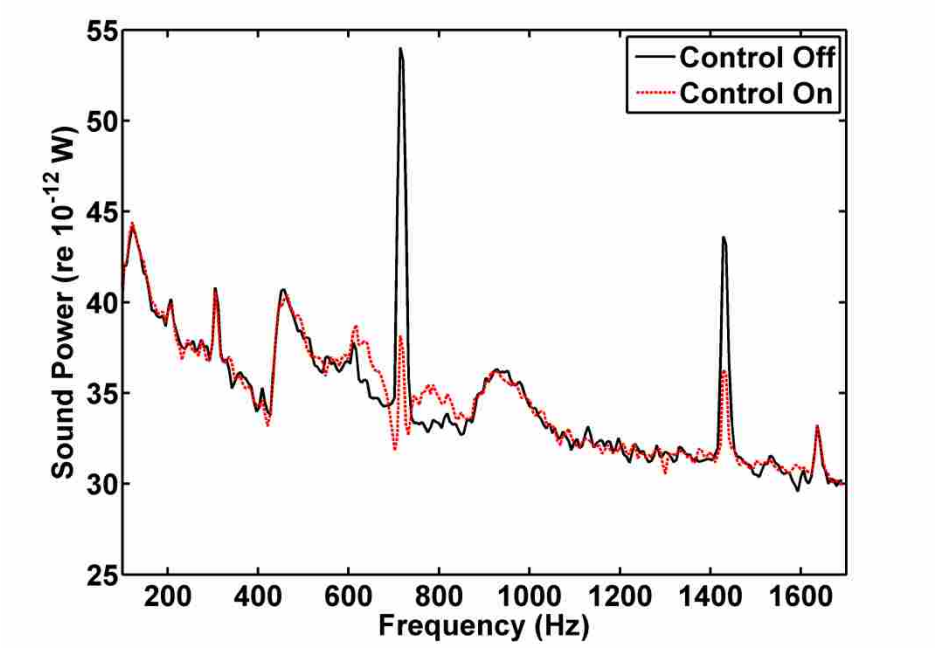

Figure 2-12: Sound power with control on and off of a two fan array using two independent three by three controller one for each fan.

The narrowband sound power spectra of one trial of the two control implementations are shown in Figs. 2-11 and 2-12. The figures show that both control systems were able to control the BPFs and the 2nd harmonics of both fans in the two fan array. The individual narrow band reduction of the BPFs and the second harmonics of each trial were determined by integrating across a 12 Hz band centered on the frequency of interest.

Two 12 Hz bands were used, the first included both BPFs and the second contained both 2nd harmonics and are reported in Table 2-2. The table shows that the narrow band reductions of the BPFs and the second harmonics of the two controller approach attenuate the BPFs an additional 1.4 dB over using a single controller and an additional 1.7 dB for the second harmonics.

Table 2-2: - 12 Hz narrow band sound power reduction (in dB) of the BPFs and 2nd harmonics of a two fan array using one control filter and two independent filters.

	1 Control Filter		*2 Control filters*	
runs	BPFs	2x BPFs	BPFs	2x BPFs
1	14.3	6.2	15.6	6.9
2	14.0	6.0	15.7	7.5
3	14.0	5.5	15.4	7.7
4	14.1	5.0	15.7	7.4
5	14.4	5.9	15.5	7.7
Average	14.2	5.7	15.6	7.4

In this case, the two controller approach outperformed the single controller for the narrow band results. In this case, the individual controllers for each fan were sufficient without using a fully coupled control system. Predicted attenuations for the two independent controllers matched what was expected at around 16 dB. However, the 6 control source implementation was limited by the shared microphone placement. Moving one microphone to make it more ideal for one fan, moves it out of the optimal place for the other fan, limiting the performance.

The directivity plots associated with these reductions are shown in 2-13 through 2-16. The plot shows the sound pressure level (SPL) in dB (re 20 μPa) in each direction with control 'on' in color and control 'off' as a wireframe mesh. The directivity plots show there was no major difference between the two control approaches in regard to directivity. The figures show that the active control attenuates the tones in all directions. Figures 2-15 through 2-16 show that there was some lobing for the two independent controllers in one direction where the single control loop is more uniform.

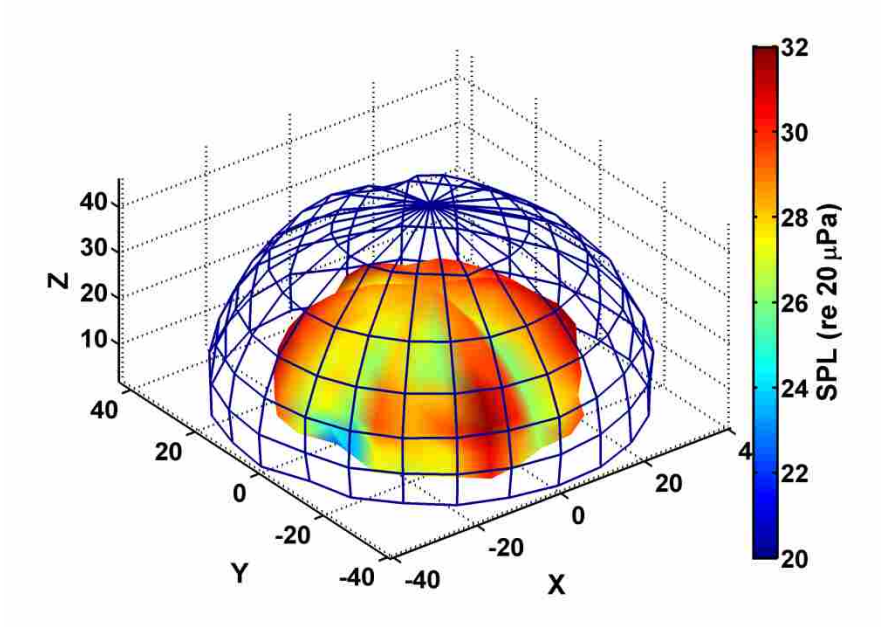

Figure 2-13: Directivity plot of a two fan array at the BPFs using one control filter with the control on (color) and control off (mesh), showing that the BPFs are reduced in all directions.

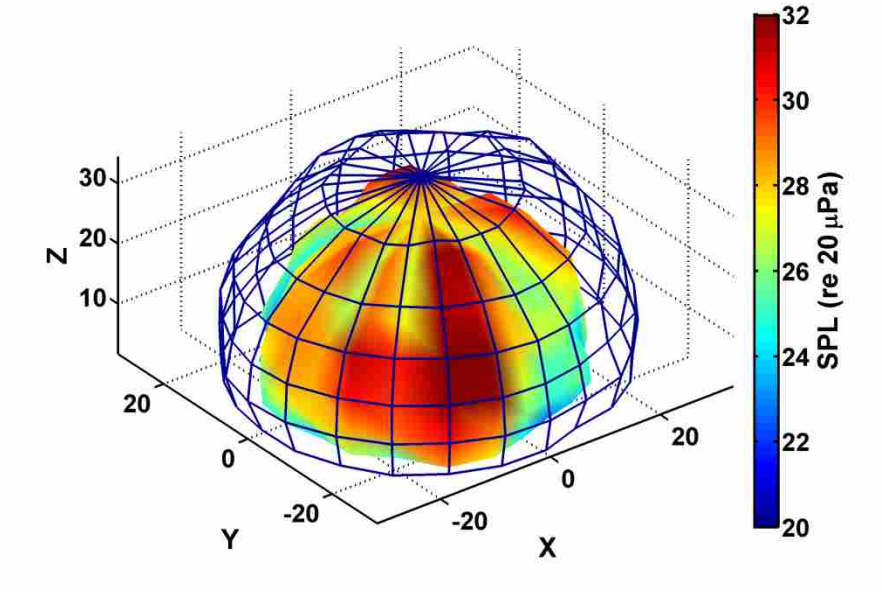

Figure 2-14: Directivity plot of a two fan array at the 2nd harmonics using one control filter with the control on (color) and control off (mesh), showing that the 2nd harmonics are reduced in all directions.

Using smaller independent controllers over larger fully coupled systems has advantages. For this case, individual controllers use less computation power than a single control loop coupled with all the control sources. Taking the number of finite impulse response filters used in the filtered-x algorithm as the metric for computation power, the one six control source by six error microphone control system used 6 control filters for the actuators in addition to the 36 (6 x 6) filters for the secondary path model, giving a total of 42 filters.

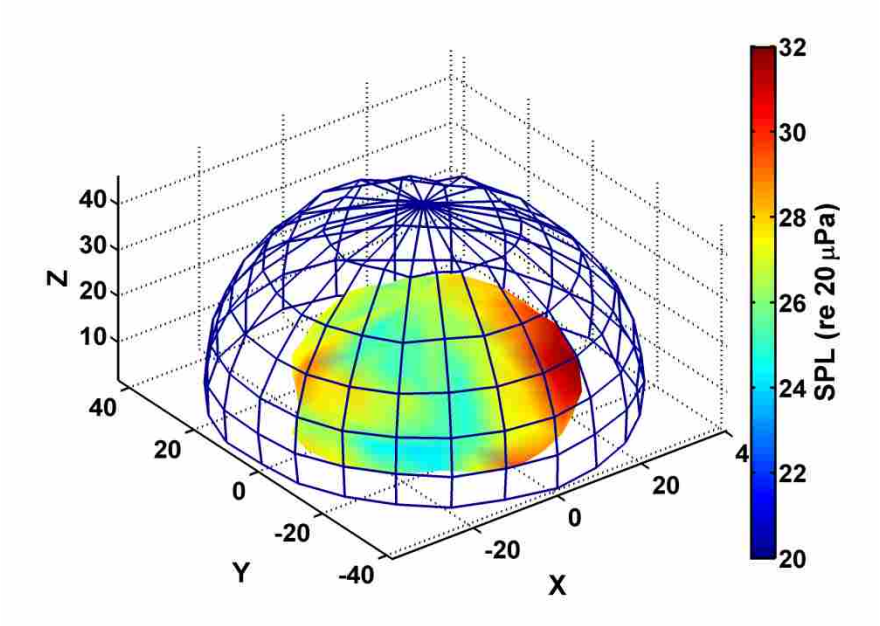

Figure 2-15: Directivity plot of the BPFs using two independent control loops to control each fan with the control on (color) and control off (mesh), showing that the BPFs are reduced in all directions.

The two control loops each used 3 control filters and 9 (3 x 3) secondary path model filters, for a total of 24 filters. Using the independent controllers required 18 fewer filters than the fully coupled system, greatly reducing the computation time. Another benefit to smaller systems is that microphones do not have to be shared between control systems. Microphones used for two different noise sources have to be placed in optimal locations for both noise sources causing limited optimal placement positions that can degrade performance.

Overall, for both control loops, the amplitude of the beat frequency was reduced significantly. Applying the active noise control to the fan array lowers the magnitude of the two BPFs to give the beat frequency the low amplitude of the two tonal components. Figure 2-17 shows a band pass filter of the time signal of a far-field microphone 1.7 m from the fan array starting with control off and showing the reduced amplitude of the beat frequency when the controller is turned on. The signal is band pass filtered to show the beat frequency better.

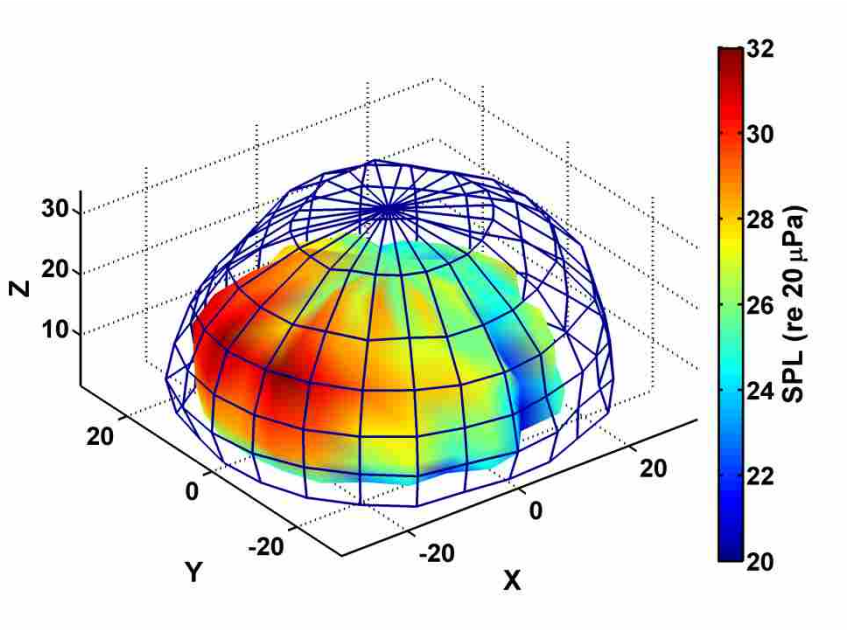

Figure 2-16: Directivity plot of the 2nd harmonics using two independent control loops to control each fan with the control on (color) and control off (mesh), showing that the 2nd harmonics are reduced in all directions.

Figure 2-17 also shows that the beat frequency appears to fluctuate around 2 Hz because of the slightly varying in rotation speeds of the two fans. Figure 16 shows that the active noise control system can be used to reduce the amplitude of the components in the beat frequency, thereby making the fan array less annoying

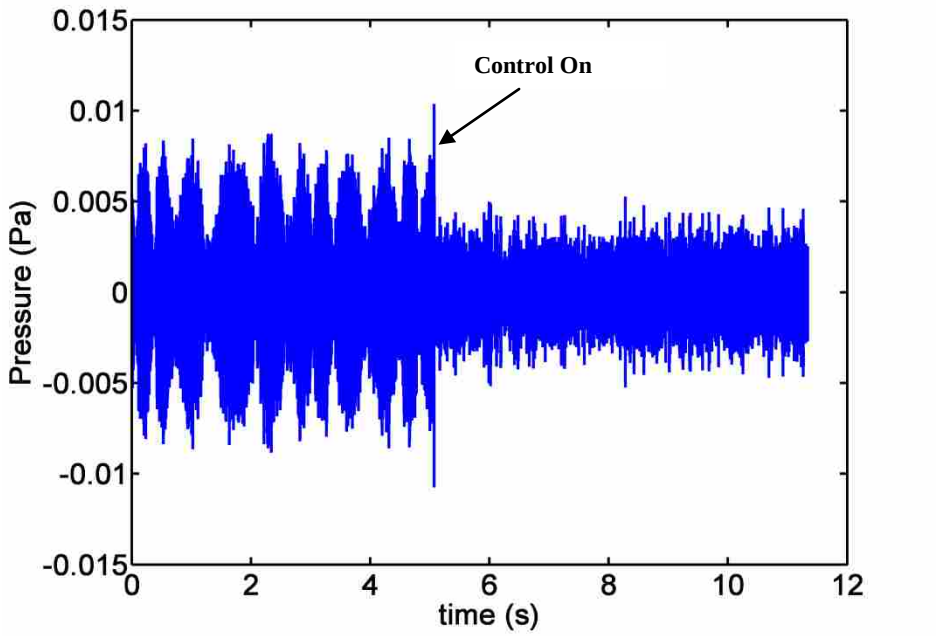

Figure 2-17: Band pass filtered time signal of a far field microphone with control off and then turned on. The noticeable beat frequency drops out of the time signal.

2.6 **Conclusion**

The active noise control of a two fan exhaust mounted array has been studied. The fan array was controlled using two different control configurations. First, a fully coupled 6 control source systems to control both fans and second, two independent controllers, one for each fan, were studied. Each fan in the array operated at different frequencies, so they were modeled individually. A single fan has two acoustic paths a direct path radiation and an acoustic path through the box and out the other fan opening. Therefore, each fan was modeled as a two source array. Since the primary source array was unknown, the sound power attenuation of various two source array was theoretically determined for the two control systems. When the second acoustic path was significant, the six control source configuration outperformed the 3 control

source configuration by 8-27 dB. However, as the relative magnitude of the second primary source dropped, the difference in performance of the two control systems was reduced until there was only 3 dB separating them. This suggests that, if the second acoustic path is significant, a control source configuration that surrounds the two fan array should be used. The source strength of the second acoustic path relative to the direct radiation was estimated to be 0.44. The microphone positions were estimated for this primary source array.

Experimental results showed that the two independent controllers actually achieved slightly more attenuation than the single control loop system. The narrow band sound power attenuation for two independent controllers was 15.6 dB for the BPFs and 7.4 dB for the second harmonics, as compared to 14.2 dB and 5.7 dB for the larger single control loop. This result suggests that using independent controller is sufficient for this two fan array. For similar implementations, this control strategy can be used for larger arrays. Additionally, using smaller independent controllers means a reduction in computation time required – in the configuration presented here, the number of filters required dropped from 42 filters to 24 filters. Additionally, the larger fully coupled system had limited optimal microphone placements for both fans, reducing the performance of the control system. The active control of the two fan array reduced the components that contributed to an audible beat frequency, thereby making it far less annoying. When control is turned on the beat frequency is no longer apparent in the time signature.

3 CHARACTERIZATION OF MICROPHONE PLACEMENT AND NOISE SENSITIVITY OF A GLOBAL ACTIVE NOISE CONTROL SYSTEM FOR A COMPACT NOISE SOURCE

3.1 **Abstract**

Optimization of active noise control systems has increased performance and applicability. Specifically, the optimization of control source placement for the active noise control of an axial cooling increased the performance but was unable to achieve the predicted gains. In this paper, the sensitivity of control systems to extraneous noise and to microphone placement errors was performed theoretically and experimentally. Two control source configurations for the sound power reduction of a simple source were analyzed by modeling the control systems. The two control source configurations compared were four symmetric control sources surrounding the noise source and an optimized linear array of four control sources. The control sources were modeled as simple sources with a baffled free space Green's function to predict the noise measured by the four error microphones. Simulation results show the linear array control source configuration is more sensitive to microphone placement errors, with a 20-33 dB reduction in attenuation for a microphone placement error of 2 mm. For the same microphone placement error the symmetric configuration resulted in a 0.8 dB drop in attenuation. Noise is then introduced to the simulation at various signals to noise ratios. Again the linear array control source configuration is more sensitive to noise. When the signal to noise ratio is 40 dB, the linear array configuration predicted attenuation is reduced by 19 dB. In contrast, the symmetric

configuration has negligible affect for the same signal to noise ratio. The experimental results suggested that for the configurations used, the sensitivity to microphone placement errors was the dominate effect. Additionally, the linear array configuration was found to be more sensitive to the microphone placement errors compared to the symmetric configuration. A 2.5 mm change in one microphone position causes an average of 6 dB loss in attenuation for the linear array configuration compared to a 0.6 dB loss for the symmetric configuration.

3.2 **Introduction**

Active noise control of axial cooling fans has been studied using various control source configurations.[18-25] The range of control system configurations includes simple single control source configurations [18-22] to four sources in various configurations[22-25]. Gee and Sommerfeldt[22-23] and Monson, et al.[35] applied a sound power reduction technique to an axial cooling fan surrounded by symmetrically-arranged loudspeakers. The sound power reduction technique was proposed by Nelson, et al.[9-10] to globally attenuate simple noise sources. The global control can be achieved by introducing control sources that are closely spaced to the primary source relative to an acoustic wavelength. Theoretically, optimal control source strengths were found by the minimization of the power radiated by the system of primary and secondary sources. In applying this technique to cooling fans, Gee found the optimal near-field error microphone locations by a) modeling all sources as monopoles, b) using the Nelson et al.[14-15] method to theoretically minimize the radiated power, and c) finding where the calculated near-field pressure level reduction was the greatest. However, because minimization of the squared-pressure at discrete locations does not necessarily guarantee the source coupling that will result in minimized radiated power, near-field measurements were used to confirm the validity of this approach.[24]

Optimization of error sensor and control source placement has been the focus of many active control studies.[27-34] For instance, Clark and Fuller[27] used an algorithm to optimize the placement of a piezoelectric actuator and strain error sensor to control the sound from a baffled simply supported plate. Berkhoff[28] found that there was an optimal distance between control sources and error sensors for the active control of sound transmission through a plate. Pulthasthan and Pota[29] used an energy based approach to find the optimal actuator and sensor locations to control structural radiation. Additionally, genetic algorithms have also been implemented to find the optimal locations for control sources and error sensors. In the specific case of axial cooling fans, Duke, et al.[30] used a genetic algorithm to improve upon the symmetric four control source arrangement used by Gee and Sommerfeldt.[22-33] The genetic algorithm results showed that including the primary source within a linear array of four control sources, two on each side of the primary source, was the optimal control source configuration that minimized the sound power of the primary source.

Experiments showed improved performance relative to Gee and Sommerfeldt's symmetric source arrangement. However, Duke, et al.[30] were not able to achieve the theoretical reductions predicted from the linear array of sources. The fact that the linear array configuration was unable to achieve the theoretical attenuations suggested that other aspects of the control system were limiting the attenuation. Snyder[16] proposed that a number of different aspects of an active control configuration impact the attenuation achieved in addition to control source configuration, including error sensor placement, quality of the reference signal and the controller. The aim in this paper was find the impact of the error sensors on the control system by simulating the control configuration used by Duke, et al.[30] compared to the symmetric control system used by Gee and Sommerfeldt.[22-23]

3.3 **Simulation**

3.3.1 Global Active Control

A brief overview of the free field active noise control theory developed by Nelson et al.[14] is presented in this section as the basis for the simulation of the control system. Free field global active noise control uses near field control sources that are closely spaced relative to a wavelength to minimize the sound power of a primary source. Each source contributes to the overall sound power and creates a radiation impedance between itself and all sources present according to

$$Z(kd) = \frac{jk^2\rho_o c}{4\pi}\left(\frac{e^{-jkd}}{kd}\right), \tag{3-1}$$

where *k* is the wave number, *d* is the distance between the two sources, ρ_o and *c* are the density and speed of sound in the medium respectively. Using equation 1, impedance matrices can then be constructed to find the total sound power of a configuration of sources. The matrix, $\overline{\boldsymbol{Z}}_{cc}$, can be defined as a control source impedance matrix between all of the control sources. Additionally, the primary source impendence matrix, $\overline{\boldsymbol{Z}}_{pp}$, would elements representing the impedances between all primary sources. Lastly, $\overline{\boldsymbol{Z}}_{cp}$ and $\overline{\boldsymbol{Z}}_{pc}$ are matrices with impedances between the primary and secondary sources where $\overline{\boldsymbol{Z}}_{cp} = \overline{\boldsymbol{Z}}_{pc}^{T}$. Using these impedance matrices to break up the sound power expression into control and primary sources, the total sound power is given by,

$$\Pi = \frac{1}{2}\left(\overline{\boldsymbol{Q}}_p^H Re\left[\overline{\boldsymbol{Z}}_{pp}\right]\overline{\boldsymbol{Q}}_p + \overline{\boldsymbol{Q}}_c^H Re\left[\overline{\boldsymbol{Z}}_{pc}\right]\overline{\boldsymbol{Q}}_p + \overline{\boldsymbol{Q}}_p^H Re\left[\overline{\boldsymbol{Z}}_{cp}\right]\overline{\boldsymbol{Q}}_c + \overline{\boldsymbol{Q}}_c^H Re[\overline{\boldsymbol{Z}}_{cc}]\overline{\boldsymbol{Q}}_c\right) \tag{3-2}$$

where $\overline{\boldsymbol{Q}}_c$ is the complex control source strength vector, whose elements are the control source strengths of each control source, $\overline{\boldsymbol{Q}}_p$ is the complex source strength vector of the primary sources, and H is the Hermitian transpose.

Defining

$$\overline{\mathbf{A}} = \frac{1}{2}\mathrm{Re}\left[\overline{\mathbf{Z}}_{\mathrm{ss}}\right], \tag{3-3}$$

$$\overline{\mathbf{B}} = \frac{1}{2}\mathrm{Re}\left[\overline{\mathbf{Z}}_{\mathrm{ps}}\right]\overline{\mathbf{Q}}_{\mathrm{p}}\,, \tag{3-4}$$

$$\mathrm{C} = \frac{1}{2}\overline{\mathbf{Q}}_{\mathrm{p}}^{\mathrm{H}}\mathrm{Re}\left[\overline{\mathbf{Z}}_{\mathrm{pp}}\right]\overline{\mathbf{Q}}_{\mathrm{p}}, \tag{3-5}$$

simplifies the sound power expression. By minimizing the sound power expression with respect to the control source strength vector, the optimal control source strengths are determined to be,

$$\overline{\mathbf{Q}}_{\mathrm{so}} = -\overline{\mathbf{A}}^{-1}\overline{\mathbf{B}} \tag{3-6}$$

with the minized sound power given as

$$\boldsymbol{\Pi}_{\mathrm{min}} = \mathrm{C} - \overline{\mathbf{B}}^{\mathrm{H}}\overline{\mathbf{A}}^{-1}\overline{\mathbf{B}}, \tag{3-7}$$

When applying the sound power minimization to a primary source using active noise control the aim is to have the control configuration achieve the minimized sound power given in Eq. 7. This approach was implemented to exhaust- mounted cooling fans by Gee and Sommerfeldt,[22-23] Monson, et al.[35] and Shafer, et al.[24] by modeling the baffled fan and control speakers as simple sources. After finding the optimal control sources that minimize the sound power, the near-field controlled pressure field relative to the primary pressure field was determined. The error microphones were placed in places of maximum attenuation, resulting in the sound power reduction of the blade passage frequencies and its harmonics. Shafer was able to confirm that the near-field pressure field relative to the primary field that was predicted was achieved.[24]

To optimize the control source configuration, Duke, et al.[30] used a genetic algorithm. The algorithm iterated through control source configurations to converge onto the optimal control source locations which minimized the sound power of a primary source. The resulting

control source configuration is shown in Fig. 1[30] compared to a surrounding configuration used by Gee, et al.[22-23] The linear array configuration predicted a reduction in the sound power of 58.4, 33.4 and 17.7 dB at 550, 1100 and 1650 Hz respectively. However, experimental results only achieved 32.4, 23.2 and 3.0 dB.[30]

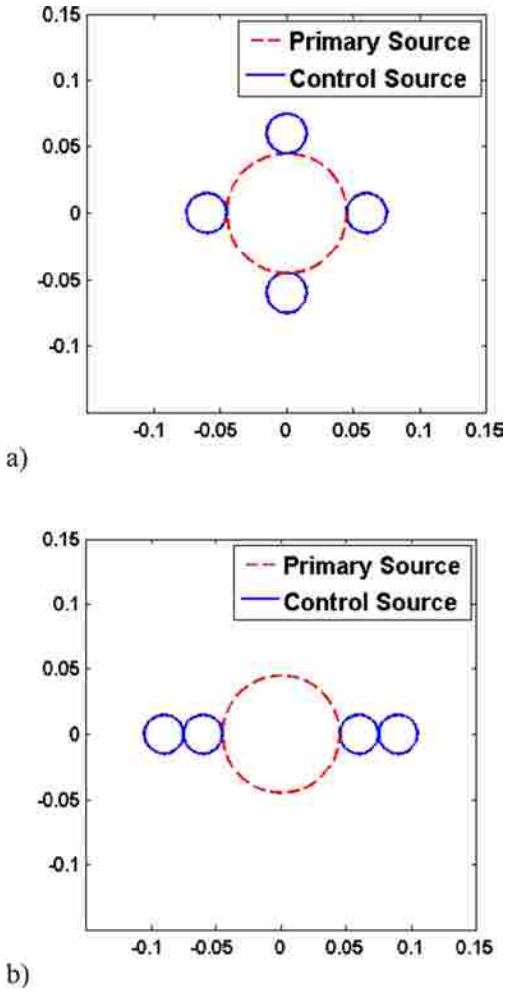

Figure 3-1: a) A symmetric configuration of control and primary sources employed by Gee, et al.[22-23] b) A linear array of control sources implemented by Duke, et al.[30] for use in global active noise control

3.3.2 Control System Modeling

In order to investigate error sensor impact on the control system, a control system model is created and used to test the control configurations under different scenarios. The model allows for the control system performance to be analyzed under different error sensor position combinations. The basis of the model is having the control sources as baffled simple sources and the microphones as point sensors. The free space Green's function for a baffled monopole source is used to model the transfer function between the simple sources and the point microphones, given by

$$G = \frac{2j\rho_o ck}{4\pi D} e^{-jkD}, \tag{3-8}$$

where *D* is the distance between the source and a point in space. The pressure due to the specific source at the chosen point is found by multiplying Eq. 3-8 by the source strength, q_s. The total pressure at point m in space can then be calculated using the Green's function between each primary and control source and point m given by,

$$P_m = q_1 G_{1m} + q_2 G_{2m} + \cdots + q_n G_{nm} \tag{3-9}$$

where G_{1m} is the Green's function between source 1 and point m. Equation 3-9 can now be used to find the pressure at each error microphone. The pressure of each microphone location is placed into a Mx1 vector, $\overline{\boldsymbol{P}}$. Separating the control and primary sources in the configuration results in,

$$\overline{\mathbf{P}} = \overline{\mathbf{G}}_{cc}\overline{\mathbf{Q}}_c + \overline{\mathbf{G}}_{pp}\overline{\mathbf{Q}}_p, \tag{3-10}$$

where $\overline{\boldsymbol{G}}_{cc}$ is a matrix of Green's functions from each control source to each of the microphones and $\overline{\boldsymbol{G}}_{pp}$is a matrix of Green's functions from each primary source to each microphone.

In order to simulate the control system, the squared pressure at each microphone location is found by forming $\overline{\boldsymbol{P}}^{H}\overline{\boldsymbol{P}}$ which results in

$$\overline{\mathbf{P}}^{\mathrm{H}}\overline{\mathbf{P}} = \overline{\mathbf{Q}}_{\mathrm{c}}^{\mathrm{H}}\overline{\mathbf{G}}_{\mathrm{cc}}^{\mathrm{H}}\overline{\mathbf{G}}_{\mathrm{cc}}\overline{\mathbf{Q}}_{\mathrm{c}} + \overline{\mathbf{Q}}_{\mathrm{c}}^{\mathrm{H}}\overline{\mathbf{G}}_{\mathrm{cc}}^{\mathrm{H}}\overline{\mathbf{G}}_{\mathrm{pp}}\overline{\mathbf{Q}}_{\mathrm{p}} + \overline{\mathbf{Q}}_{\mathrm{p}}^{\mathrm{H}}\overline{\mathbf{G}}_{\mathrm{pp}}^{\mathrm{H}}\overline{\mathbf{G}}_{\mathrm{cc}}\overline{\mathbf{Q}}_{\mathrm{c}} + \overline{\mathbf{Q}}_{\mathrm{p}}^{\mathrm{H}}\overline{\mathbf{G}}_{\mathrm{pp}}^{\mathrm{H}}\overline{\mathbf{G}}_{\mathrm{pp}}\overline{\mathbf{Q}}_{\mathrm{p}} \quad (3\text{-}11)$$

In order to minimize the squared pressure at the microphone, like an active noise control system, the derivative of Eqn. 3-11 is taken with respect to $\overline{\boldsymbol{Q}}_{c}$ to yield

$$\frac{\partial\overline{\mathbf{P}}^{\mathrm{H}}\overline{\mathbf{P}}}{\partial\overline{\mathbf{Q}}_{\mathrm{c}}} = \overline{\mathbf{G}}_{\mathrm{cc}}^{\mathrm{H}}\overline{\mathbf{G}}_{\mathrm{cc}}\overline{\mathbf{Q}}_{\mathrm{c}} + \overline{\mathbf{G}}_{\mathrm{cc}}^{\mathrm{H}}\overline{\mathbf{G}}_{\mathrm{pp}}\overline{\mathbf{Q}}_{\mathrm{p}} \quad (3\text{-}12)$$

The derivative is set to zero and the control source strengths are solved for, resulting in

$$\overline{\boldsymbol{Q}}_{c} = -(\overline{\boldsymbol{G}}_{cc}^{H}\overline{\boldsymbol{G}}_{cc})^{-1}\left(\overline{\boldsymbol{G}}_{cc}^{H}\overline{\boldsymbol{G}}_{pp}\overline{\boldsymbol{Q}}_{p}\right). \quad (3\text{-}13)$$

Equation 3-13 gives the source strengths the control system will converge to with the microphones in any configuration. These control source strengths are then used to find the sound power of the control system configuration using Eq. 3-2. The attenuation of the primary source field is then calculated. Thus, by using this model, the attenuation achieved by a control system can be found by virtue of the microphone positions.

3.3.3 Control System Simulation

The control system is simulated, using the presented model, for the two control configurations shown in Fig. 3-1., the optimized linear array of control sources and the symmetric configuration. With the microphones in the optimal locations, Shafer, et al.[25] confirmed that the near-field controlled pressure relative to the primary pressure was created by the control system for the symmetric configuration. Building upon Shafer's work, the sound power of a primary source operating at 600 Hz was simulated with the two different control configurations. For the simulation, the error microphones are placed in the optimal locations

found by Gee, et al.[22-23,25], which results in maximum attenuation of 58 dB for the linear array and 29 dB for the symmetric configuration.

After confirming the control configurations could achieve the predicted maximums, the simulation is now used to find the sensitivity of the two control systems relative to microphone placement error. In the simulation, a single microphone is moved with three of the four microphones remaining placed in the optimal locations. The single microphone is moved along a line in space which crosses the optimal location. The movement path of the microphone and the near-field controlled pressure relative to the primary field for both configurations are shown in Figs. 3-2 and 3-3. A total of three error microphone simulations are performed, one for the symmetric case and since the linear array has two speakers closer to and two farther from the primary source, two different microphone paths were simulated, giving a total of three different simulations.

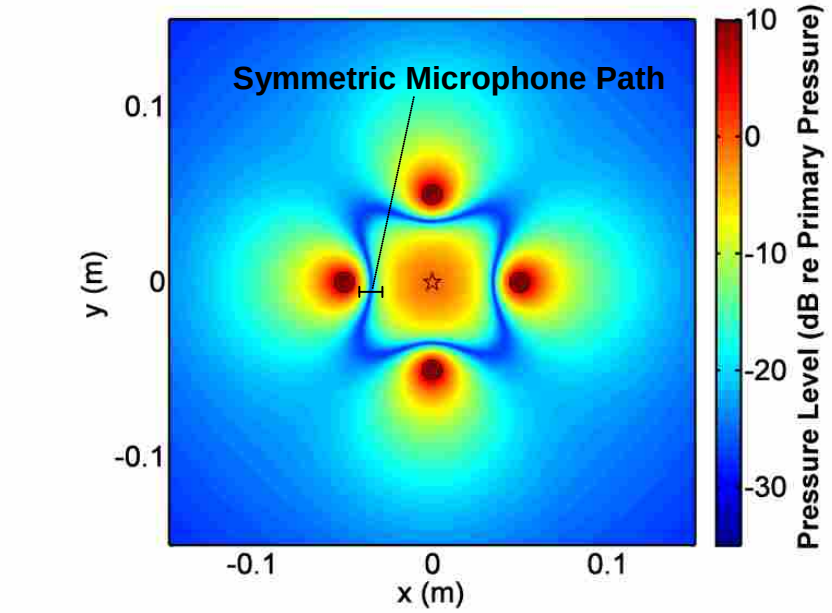

Figure 3-2: Near-field controlled pressure field relative to the primary field (in dB) for the symmetric configuration of control sources, with the circles as control sources and the star as the primary source. The microphone path used for the non-fixed microphone shown as the line that crosses the contour of maximum attenuation.

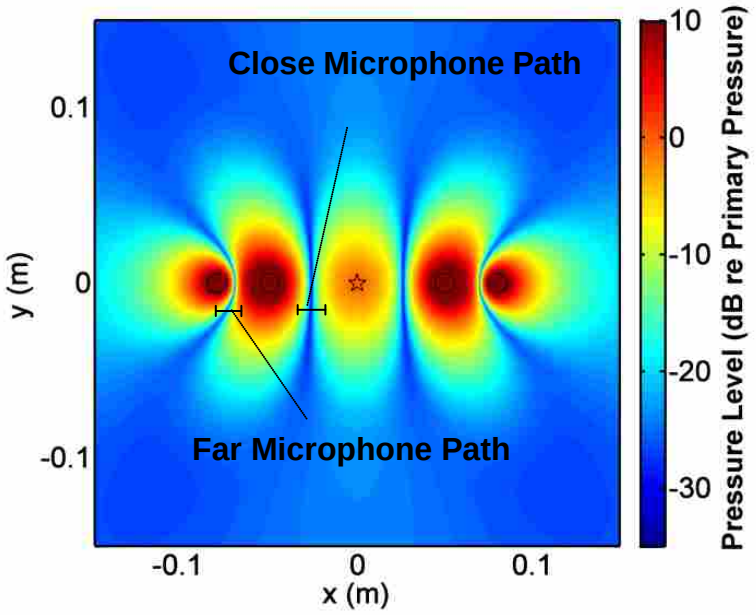

Figure 3-3 Near-field controlled pressure field relative to the primary field (in dB) for the linear configuration of control sources, with the circles as control sources and the star as the primary source. The microphone path used for the non-fixed microphone shown as the line that crosses the contour of maximum attenuation. The linear configuration has two simulations, one for the close microphone path and one for the far microphone path.

All the paths start 1 cm from the optimal location and move 1 cm past the optimal placement, with a total movement of 2 cm per simulation.

Figure 3-4 shows the results of the single microphone placement error simulation, with distance on abscissa corresponding to the distance from the ideal placement and with the positive values being further from the primary source. For the two linear configuration microphone placement plots, there is a large, narrow peak in the predicted attenuation, creating a wide range of possible sound power attenuations for small errors in microphone placement. The microphone closer to the primary source leads to attenuation variations from 15 – 60 dB, while the predicted attenuation for the microphone farther from the primary source varies from 19 – 60 dB for the 2 cm simulation. Additionally, the peak in the attenuation is narrow for the linear configuration, meaning a microphone placement error of 2 mm from the ideal placement means a 25-33 dB

drop in sound power attenuation. In contrast, the surrounding configuration varies from 20 – 30 dB across the 2 cm simulation, which is a relatively small range compared to the linear configuration. In particular, a 2 mm error in placement of one microphone from the ideal placement only yields a 0.8 dB decrease in attenuation compared to the large decrease of 25-33 dB for the linear array control configuration.

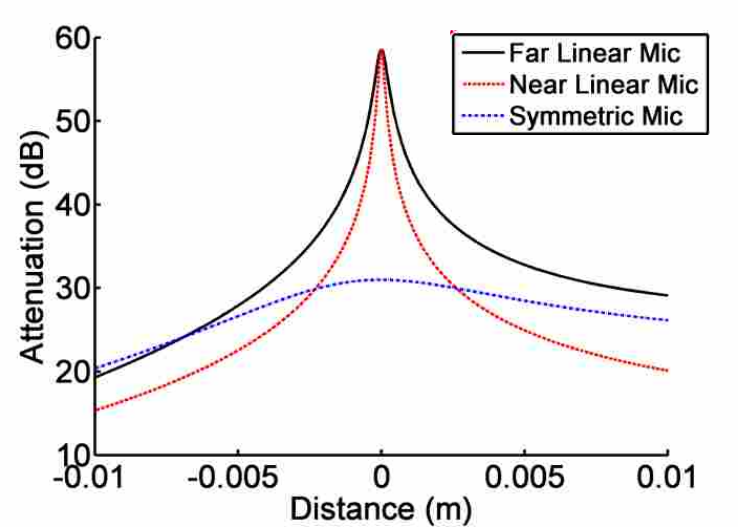

Figure 3-4: The simulated sound power attenuation of a primary source (in dB) for three simulations. One microphone is moved along the paths shown in Figs. 3-2 and 3-3 while keeping the other microphones stationary, with the abscissa being distance from the optimal microphone position.

Since these control systems use four microphones, the above simulation is repeated incorporating position errors of all the microphones. As before, one of the four microphones is moved along the same line in space, as shown in Figs. 3-2 and Fig. 3-3, which is referred to as the simulation microphone. For all three simulations, this microphone is referred to as the simulation microphone. The other three error microphones are given an error corresponding to a 1 mm x 1 mm grid broken up into 81 different positions, with each grid centered on the ideal microphone location. At each increment of the simulation microphone, the other three

microphones are individually incremented across their grid to give to give a total of 531,441 microphone position combinations. The attenuation is calculated for all these microphone position combinations with the maximum and minimum attenuation being saved at each increment of the simulation microphone. The maximum and minimum attenuations give an extreme range of expected values from the control system based on 1 mm error in placement of all the microphones. The results are plotted in Figs. 3-5 through 3-7 along with the curves from the previous single microphone placement error simulations for all three simulation paths. Looking at Figs. 3-5 through 3-7, there is a large variability in possible attenuation values for the linear array configuration. Specifically, when the simulation microphone is near the optimal location, where the horizontal axis is close to zero, the attenuation has a range of 22-23 dB for the linear array control configuration. The large range shows how sensitive this configuration is to microphone position errors especially compared 0.4 dB range of expected values for the symmetric case. Looking further into the two linear array configuration simulations, there is more variability associated with the far microphone compared to the close microphone, specifically, the far microphone has a 23 dB spread at the ideal placement position compared to 22 dB range for the near microphone. Additionally, when the simulation microphone was past the optimal location, i.e., farther from the primary source, there is a 5 dB spread in the attenuation for the far microphone compared to a 2 dB spread for the linear near microphone. The results show that the sensitivity of the linear array control system configuration to microphone placement errors is much greater than that of the symmetric control system configuration.

Moving on from the placement error simulations, the effect of having an area sensor instead of a point sensor is investigated.

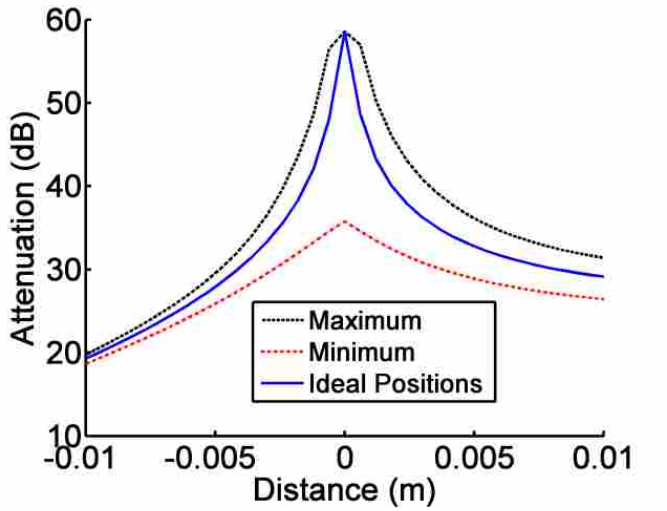

Figure 3-5: The simulated sound power attenuation for moving the far microphone in the linear configuration across the path shown in Figure 3-3 and for the other three microphones having position errors of 1 mm in the x and the y direction so the maximum and minimum sound power attenuation curves correspond to the extreme results obtained for these simulations.

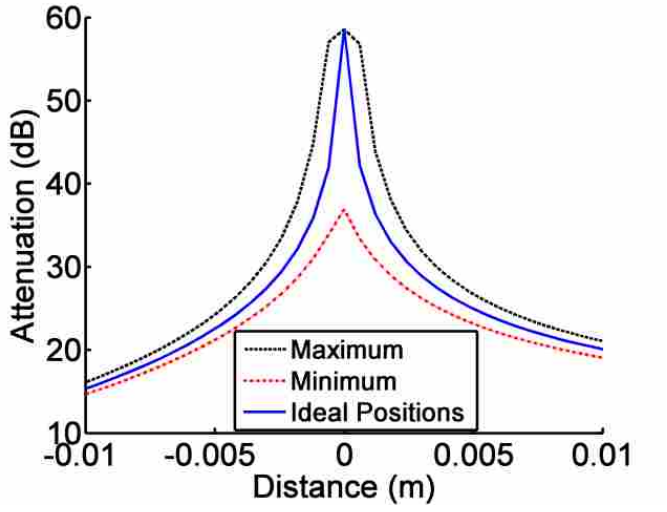

Figure 3-6: The simulated sound power attenuation for moving the near microphone in the linear configuration across the path shown in Figure 3-3 and for the other three microphones having position errors of 1 mm in the x and the y direction so the maximum and minimum sound power attenuation curves correspond to the extreme results obtained for these simulations.

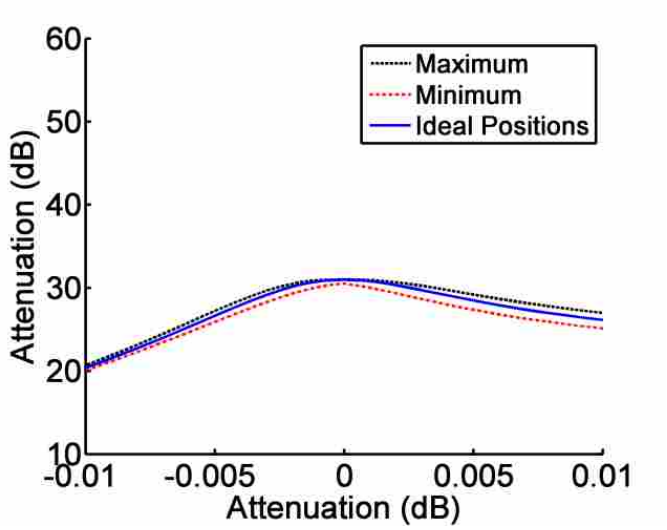

Figure 3-7: The simulated sound power attenuation for moving the microphone in the symmetric configuration across the path shown in Figure 3-2 and for the other three microphones having position errors of 1 mm in the x and the y direction so the maximum and minimum sound power attenuation curves correspond to the extreme results obtained for these simulations.

The sharp peak in predicted attenuation for the linear array configuration because of placement error suggested that the microphone diaphragm size might have an impact on performance of the control system. The model is changed from having point sensors to area sensors.

The free space Green's function is modified to include a surface integral of the pressure across each microphone diaphragm, with an area of 5 mm by 5 mm for each diaphragm. The same process is used to solve for the control source strengths and resulting sound power with the modified Green's functions as previously presented. Performing the simulation with all four microphones in the ideal locations, the results showed that for this microphone diaphragm size, the sound power attenuation does not change, i.e., giving the same results as when the point error sensors were used in the model. The control system simulation created a node in the pressure across the center of the microphone with positive and negative pressure on either side of the node. The result suggests that the size of the diaphragm was not as critical in the control system as the location of the acoustic center of the microphone.

The last aspect of the error sensor sensitivity that was investigated was sensitivity to noisy signals used for active noise control. The noise would come from either electrical noise from the equipment or acoustical noise at the error sensor. The noise is added to the system at the error microphones with the form of

$$\mathrm{n} = \mathrm{A}e^{-2\pi \mathrm{bi}} \tag{3-11}$$

where A is an amplitude term which can be varied to added different signal to noise ratios and b is a random number with a uniform distribution to give the noise a random phase element. So, Eqn. 3-9, the pressure at each microphone, was modified to include a noise vector, whose elements are representative of the noise each error microphone, Eqn. 3-11, given by,

$$\overline{\boldsymbol{P}} = \overline{\boldsymbol{G}}_{cc}\overline{\boldsymbol{Q}}_c + \overline{\boldsymbol{G}}_{pp}\overline{\boldsymbol{Q}}_p + \overline{\boldsymbol{n}}. \tag{3-12}$$

Now following the same procedure above, minimizing the squared pressure at each of the microphones results in the control source strengths,

$$\overline{\boldsymbol{Q}}_c = -(\overline{\boldsymbol{G}}_{cc}^H\overline{\boldsymbol{G}}_{cc})^{-1}\left(\overline{\boldsymbol{G}}_{cc}^H\overline{\boldsymbol{G}}_{pp}\overline{\boldsymbol{Q}}_p + \overline{\boldsymbol{G}}_{cc}^H\overline{\boldsymbol{n}}\right). \tag{3-13}$$

Equation 3-13 shows that when the noise is added at the error sensor, it is filtered by the Hermitian transpose of the control source transfer function from the source to the microphone. The control source strength is then put back into the equation for the total sound power of the system, Eqn. 3-2, in order to determine the attenuation of the primary source sound power. The effect of different signal to noise ratios on the control system is found by adding the noise 100 times and finding the average sound power attenuation. In this simulation, the microphones are still incremented through the paths shown in Figs. 3-2 and 3-3. At each microphone position on the microphone path normally distributed noise was added to the control source strengths 100 times, the sound power for each simulation was calculated, and the 100 sound power attenuations were averaged. Noise corresponding to different signal to noise ratios is used in the simulations.

The signal to noise ratios is calculated by finding the pressure at each microphone from the primary source compared to the added noise. The results are shown in Figure 3-8 and 3-9.

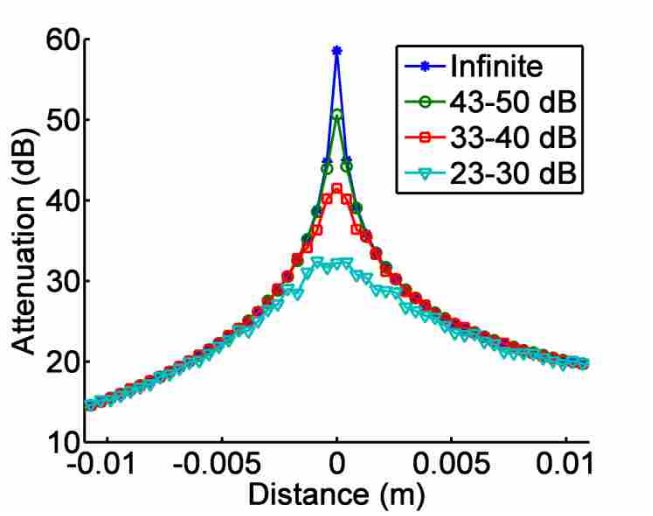

Figure 3-8: The placement sensitivity of the near microphone for the linear array with noise corresponding to different signal to noise ratios added at the error microphone and the resulting averaged sound power attenuation.

As shown, the noise in the control system has a much greater effect on the linear configuration. The attenuation dropped from 59 dB to 41 dB for a 40 dB signal to noise ratio used compared to an infinite signal to noise ratio. Looking at the symmetric configuration, there is virtually no drop for the symmetric case with the same 40 dB signal to noise ratio. Looking further into the linear array case, the control configuration is more sensitive to the noise when the microphone is closer to the optimal location (close to zero on the abscissa).

The overall results show the linear array control system configuration was more sensitive to uncorrelated noise sources compared to the symmetric control system configuration. Additionally, the linear array control configuration is much more sensitive to noise and microphone placement than the symmetric configuration.

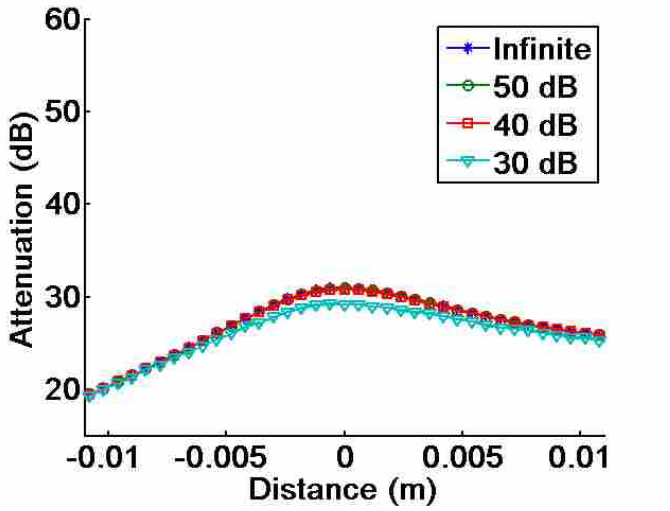

Figure 3-9: The placement sensitivity of the symmetric microphone for the linear array with noise corresponding to different signal to noise ratios added at the error microphone and the resulting averaged sound power attenuation.

3.4 Experiments

3.4.1 Experimental Setup

The microphone placement sensitivity of the two configurations is now tested experimentally. The primary source used is a 2.5 cm tweeter loudspeaker placed in a speaker plate. The 2.5 cm control sources were placed around the primary source according to Fig. 3-1 for both configurations and the control set up is shown in Fig. 3-10. The feed-forward control system is implemented using a Texas Instruments 320c6713 DSP with a sampling frequency of 4000 Hz. The controller used 20 control filter coefficients and 20 secondary path model coefficients. The error microphones are 6mm Hosiden electret microphones. Anti-aliasing low-pass filters are Krohn-Hite 3384 8 pole filters set with a cutoff frequency of 1800 Hz.

- 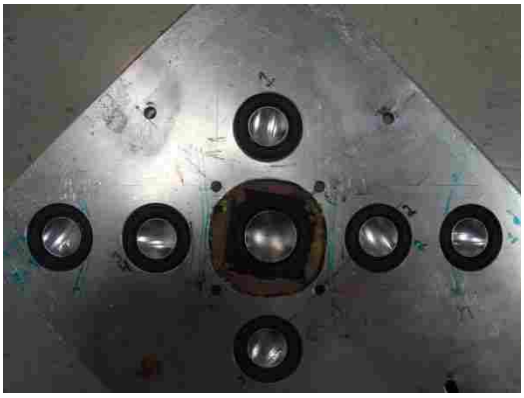

Figure 3-10: The experimental setup of the linear array and symmetric control configurations used.

The primary source speaker is driven at 600 Hz. The sensitivity of the control system to microphone location is found by placing three of the four microphones in the optimal locations. Following the control paths in Figs. 3-2 and 3-3, the fourth microphone is incremented at 2.5 mm increments with a total of 9 measurements. Each error microphone path is tested four times. At each error sensor location, the sound power attenuation of the primary field was measured. The sound power measurement is obtained using a rotating semicircular array with a radius of 1.8 m and with thirteen 12.7mm GRAS type I microphones equally spaced along the semicircle. The control set up is placed directly under the center microphone of the array and the array is rotated about the center microphone at 15 degree increments to create a 360 degree hemispherical scan. At each microphone location, the autospectrum is calculated using 15 averages and a frequency resolution of 6.1 Hz. The sound power is then calculated using an area weighting function used by Monson, et al.[35] In this method, an area weighting function is used on the individual microphones measurements to account for the unequal areas swept out by the measurement array to determine the sound power. Additionally, control is also run using 12.7 mm type I Larson

Davis microphones to test whether the surface area of the microphone diaphragm was experimentally an important factor in sound power attenuation of the primary source. The larger microphones were placed in the maximum attenuation locations for this trial.

3.4.2 Results and Discussion

The results for the 4 trials of sensitivity to error sensor placement are shown in Figs. 3-11 through 3-13. The experimental trials are plotted along with the simulated range for possible attenuations calculated in Figs. 3-5 through 3-7.

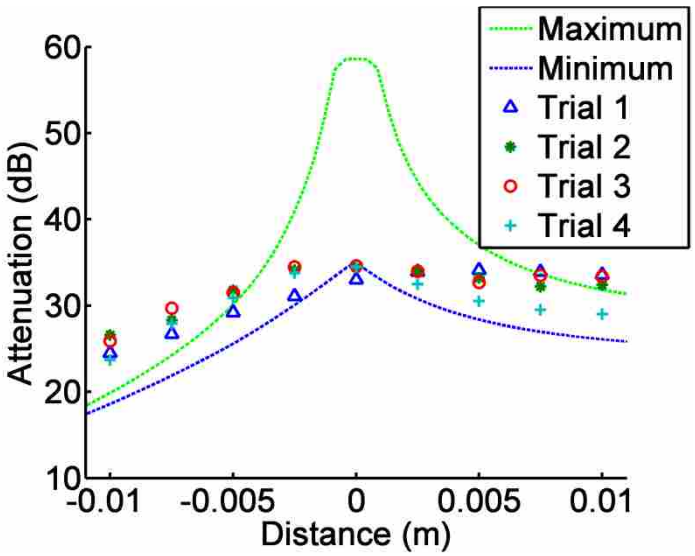

Figure 3-11: The experimental results from the 4 trials of the linear array configuration far microphone plotted against the possible theoretical result range of possible sound power attenuation taken from fig. 3-5.

Generally the values are within the range predicted by Figs. 3-5 through 3-7. However, toward the optimal position placement of the moved microphone, the values become closer to the minimum predicted attenuation.

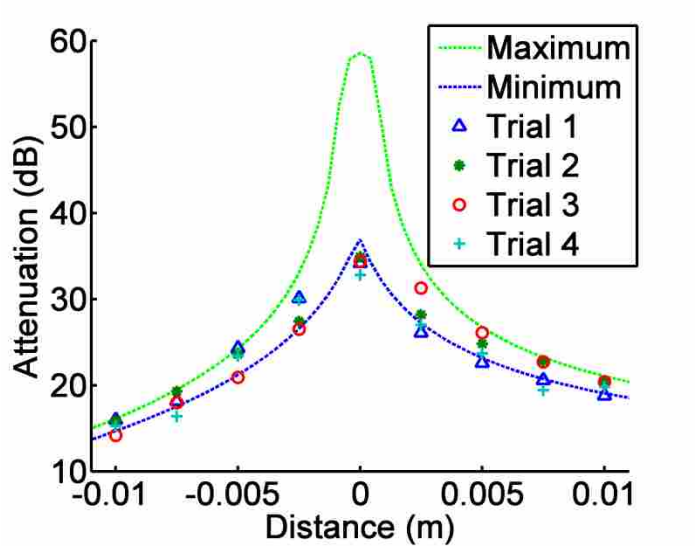

Figure 3-12: The experimental results from the 4 trials of the linear array configuration near microphone plotted against the possible theoretical result range of possible sound power attenuation taken from fig. 3-6.

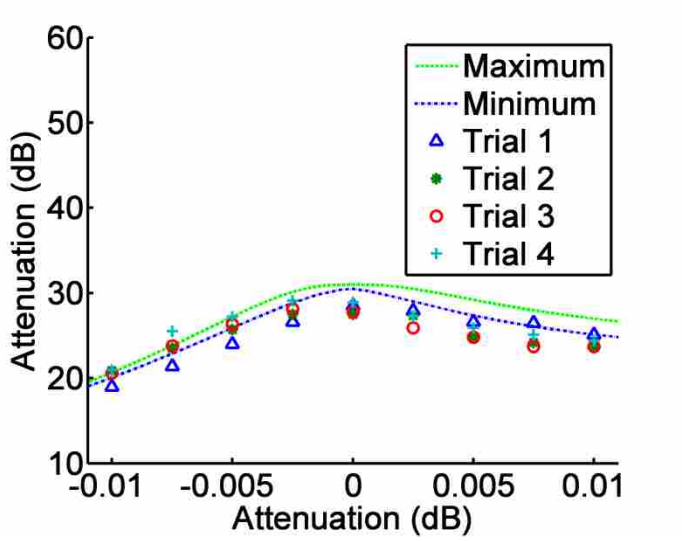

Figure 3-13: The experimental results from the 4 trials of the symmetric configuration plotted against the possible theoretical result range of possible sound power attenuation taken from fig. 3-7.

As for the linear array configuration plots, the far microphone has experimental values that are higher than predicted on the outside tails of the plot. However, the shape experimental trials for the far microphone still peak at the optimal location, sloping downward faster as the

microphone moves from the optimal location toward the primary source than when the microphone is moving away from the primary source. This pattern matches the pattern of the simulation shown in Fig. 3-4 when 3 of the 4 microphones are in the optimal locations. Allowing for an experimental error 1 mm in regards for all four microphones, the data matches what could be reasonably expected from the control system, meaning that most of the data is within the expected range calculated and shown in Figs. 3-5 through 3-7. The experimental results showed that the linear array did have a greater sensitivity to microphone placement compared to the symmetric configuration. Looking specifically across the 9 measurements for a single trial (moving one microphone 2 cm) the range of sound power attenuation values for the closer microphone in the linear array configuration was 18-34 dB. This 16 dB range was much higher than the symmetric configuration that had a range of 4 dB (24-28 dB). Specifically, moving off the optimal location in either direction 2.5 mm meant an average of 5.5 dB lost attenuation for the closer microphone in the linear array configuration compared to 0.6 dB for the symmetric configuration for the same microphone movement.

The error sensor signal to noise ratio is determined by taking a measurement with the control on and off. The signal to noise ratio was determined to be 50-70 dB for the four microphones. The noise simulation plots show that a signal to noise ratio of 50-70 dB did not have a significant impact on either control configuration. The signal to noise ratio measurement and the experimental results from moving one microphone across the optima results suggests that microphone placement is the most important factor in achieving the maximum sound power attenuation and not noise sources for this configuration

When 12.7 mm microphones were used as error sensors for the linear array configuration, the amount of control achieved matched 6mm microphones of 33.1 dB sound power reduction.

The result of 33.1 dB using the larger microphone diaphragm as error sensors confirms the simulation result that microphone diaphragm size does not affect the control at this frequency.

3.5 **Conclusion**

The purpose of this paper was to investigate the sensitivity of two different control configurations in regard to error microphone position errors and the sensitivity of the control systems to added noise. The two control systems simulated were a symmetric 4 control source configuration that surrounded the primary source and a linear array of 4 control sources with the primary source in the middle of the array. The control systems were modeled using baffled free space Green's functions as the transfer function between the primary and control sources to the microphones. Using this model, simulations were performed. The simulated results showed that linear array has more sensitivity than the symmetric case with regard to error sensor placement and to extraneous noise sources. A 2.5 millimeter change in microphone position caused a 25-30 dB theoretical loss in attenuation compared to a 2 dB loss for the symmetric case. For the noise source simulation, adding noise to the simulation greatly affected the linear case with a minimal effect for the symmetric configuration. A 40 dB signal to noise ratio for the control source strengths resulted in a decrease in attenuation from 59 to 41 dB for the linear array configuration.

The experimental results confirmed that the linear array configuration was more sensitive to microphone placement with large decreases in attenuation based on microphone placement error. A 2.5 mm change in the position a single microphone cause an average 5.5 dB loss in sound power attenuation for the linear array configuration compared to an average loss of 0.6 dB for the symmetric case. A measurement of the signal to noise ratios at the error microphones showed that in this experimental configuration, noise was not a significant factor for the control

systems. The acoustic center of the microphone proved to be the most important part of the control because microphone diaphragm size did not affect the global control results both theoretically and experimentally. Overall, the results show that the control configuration can have an impact on the robust nature of the control system including sensitivity to microphone placement, noise sources, and model errors. Since the control source configuration has an impact on the sensitivity of a control system to noise and error sensor placement, the shape of the error sensor placement curve should be used to constrain the optimization.

4 CONCLUSIONS

4.1 Summary

The theoretical modeling of the active noise control and experimentation of a two fan array was performed. Each fan in the array was modeled as a simple source and was actively controlled using two different control source configurations. Since the blade passage frequency was at slightly different frequencies for each fan, each fan was modeled individually. However, the presence of the second fan created a second acoustic path to the far field, such that each fan could be considered as a two primary source array. The fan array was controlled with a single control filter with 6 control sources and 6 error sensors. Additionally, each fan in the array was controlled with its own independent control filter with 3 control sources and 3 error sensors. The experimental results showed that using individual control systems, one for each fan, was a better control approach. The result suggests, that each fan on the array then can be modeled individually, meaning that additional fans can be added to the array and controlled by using nearby control sources and error sensors. In addition to allowing for larger fan arrays, using two smaller control systems instead of one large controller means a reduced computation cost for the digital signal processor. The six by six control filter had 42 finite impulse response filters while two independent controllers had 24 filters. The amplitudes of the tones at the BPFs of the multiple fan array were attenuated by about 15 dB for a narrow band of 12 Hz centered on the

BPFs. Additionally, the amplitude of the second harmonics of the fan array were reduced by 6 dB. The attenuation of the peak amplitudes of the BPF of each fan caused the beat frequency to correspond to the low amplitude of the components and was no longer noticeable in the time signature of a far field microphone.

The sensitivity of two different near-field source configurations was analyzed for the active control of a single monopole source. The first configuration was a symmetric four control source configuration surrounding the primary source. The second control configuration was a linear array of four control sources with the primary source in the middle of the array. The linear array of control sources has large theoretical attenuation values but was unable to achieve the attenuation experimentally. The control system was simulated by modeling each source with a baffled free space Green's function and the microphones were modeled as point sensors. Different parameters were changed to find factors that might be impacting the experimental results, including microphone placement and extraneous noise sources.

The linear array proved to be more sensitive to microphone position. A 2 mm error in the position of one microphone created a 20-33 dB drop in the theoretical sound power attenuation. Incorporation of the position errors for all microphones in the control system showed that a wide range of possible attenuations was possible. In contrast, errors in the symmetric configuration saw slight reductions in attenuation based on microphone positions with only a 0.8 dB reduction in attenuation for a microphone placement error of 2 mm.

Sensitivity of the two configurations was tested by adding uncorrelated noise at the error microphone. Noise was added to the system at different signal to noise ratios. At 40 dB, the predicted attenuation dropped by 17 dB for the linear configuration but negligibly affected the symmetric case. The surface area of the error microphones was also investigated using the

simulation because the sharp peak in attenuation for the linear array control configuration based on error sensor placement suggested that maybe microphone diameter size could be a limiting factor. However, the surface area of the control microphones did not affect the predicted sound power attenuation and this result was confirmed by experimentation. The placement of the acoustic center in the right location was the determining factor in the amount of control achieved by the control system.

Experimental testing of the two configurations showed that external noise sources were not an important factor for this set up. Microphone positions errors were the dominant factor limiting the attenuation for both control configurations. Across the 2 cm in microphone position error that was tested, the linear array configuration ranged from 18-34 dB, a 16 dB spread. In contrast, the symmetric configuration ranged from 24 to 28 dB. Additionally, a 2.5 mm change in one microphone position off the optimal location caused an average 5.5 dB drop for the linear configuration and only 0.6 dB reduction in attenuation for the symmetric configuration. The linear array control configuration proved to be more sensitive to microphone error sensor placement both theoretically and experimentally.

4.2 **Recommendations**

The study of a two fan array was for an exhaust-mounted array. However, fan arrays are sometimes used inside an enclosure such as a computer server. Internal fans provide a different acoustic environment which cannot be modeled as a source radiating into free space. Additional problems facing internal fan applications include, having a small foot print, a computer server does not allow a lot of room for control actuators to be placed.

A second recommendation is to apply the sensitivity analysis as a constraint to optimization routines. The simulation of the linear array configuration showed that microphone placement sensitivity was the limiting factor. Dramatic changes in attenuation based on small microphone placement errors, characteristic of the linear array configuration were found to be undesirable. Using the derivative of the sensitivity curve as a constraint would allow for a configuration that has gradual changes in attenuation based on microphone placement like the symmetric configuration.

REFERENCES

1. L. Huang, “Characterizing computer cooling fan noise”, *J. Acoust. Soc. Am*., **114**, 3189-3200, (2003).

2. I. J. Sharland, “Sources of noise in axial flow fan”, *J. Sound Vib*. **1**(3), 302-322, 1964.

3. M. Cudina, “Noise generation in vane axial fans due to rotating stall and surge” Proc. Insn. Mech. Engrs., **215**, part C 57-64 (2001).

4. K. B. Washburn, G. C. Lauchle, “Inlet flow conditions and tonal sound radiation from a subsonic fan”, *Noise Control Eng. J*. **31** (2) 101-110. (1998).

5. R. E. Longhouse, “Vortex shedding noise of low tip speed, axial flow fan,” *J. Sound Vib.* **53**, 25-46 (1978).

6. W. Chic, G.C. Lauchle, D.E. Thompson, “Subsonic axial flow fan noise and unsteady rotor force,” *J. Acoust. Soc. Am*., **85**(2), 641-647, (1989).

7. J. Fitzgerald, G.C. Lauchle, “Reduction of discrete frequency in small, subsonic axial-flow fans”, *J. Acoust. Soc. Am*. **76**, (1984).

8. H. Shin, H. Sun, Hyosung, S. Lee, “Development of a new free wake model considering a blade–vane interaction for a low noise axial fan planform optimization” *J. Sound Vib*., **291**, 503–515,(2006).

9. N. Le S. Filleul," An investigation of axial-flow fan noise," *J. Sound Vib*., **3**, 146-165 (1966).

10. P. Lueg, “Process of silencing sound oscillations” US 2043416, (1936).

11. S. M. KUO, D. Morgan, “Active noise control: a tutorial review”, *Proceeding of the IEEE*, **87**(6), (1999).

12. B. Widrow and S. D. Stearns, “Adaptive signal processing”. Englewood Cliffs, NJ: Prentice-Hall. (1985).

13. S. D. Sommerfeldt, P.J. Nahsif, “An adaptive filtered-x algorithm for energy-based active control” *J. Acoust. Soc. Am*. **86** (1), (1994).

14. P. A. Nelson, A. R. D. Curtis, S. J. Elliott and A. J. Bullmore, "The minimum power output of free field point sources and the active control of sound", *J. Sound Vib.*, **116**, pp. 397–414, (1987).

15. S. J. Elliot, P. Joseph, P. A. Helson and M. E. Johnson, "Power output minimization and power absorption in the active control of sound", *J. Acoust. Soc. Am.*, **90**, pp. 2501–2512, (1991).

16. S. D. Snyder, "Acitve control – a bigger microprocessor is not always enough", *Noise Control Eng. J* **49** (1) pp. 21-29, (2001).

17. Hanson, Snyder, Acitive control of Sound and Vibration. E&FN Spon; London (1997).

18. D. A. Quinlan. "Application of active control to axial flow fans," *Noise Control Eng. J.* **39**, pp.95-101, (1992).

19. J. Wang, L. Huang, L. Cheng, "A study of active tonal noise control for a small axial flow fan", *J. Acoust. Soc. Am.*, **117**(2): pp. 734-43, (2004).

20. J. Wang, L, Huang, "Active control of drag noise from a small axial flow fan", *J. Acoust. Soc. Am.* **120**(1), pp. 192-203, (2006).

21. G. C. Lauchle, J. R. MacGillivray, D. C. Swanson, "Active control of axial-flow fan noise", *J. Acoust. Soc. Am.*, **101**, pp. 341-349, (1996).

22. K. L. Gee, S. D. Sommerfeldt, , "Application of theoretical modeling to multichannel active control of cooling fan noise", *J. Acoust. Soc. Am.* **115**, pp. 228-336,(2004).

23. K. L. Gee and S. D. Sommerfeldt, "A compact active control implementation for axial cooling fan noise," *Noise Control Eng. J.* **51**(6), 325–334, (2003).

24. B. M. Shafer, K. L. Gee, S. D. Sommerfeldt, "Verification of a near-field error sensor placement method in active control of compact noise sources", *J. Acoust. Soc. Am.*, **127**, EL66-EL72, (2010).

25. B. Abali, S. Guthridge, R. Harper, P. Manson, "Mutual active cancellation of fan noise and vibration".United States Patent Publication, US 7,282,873 B1, (2007).

26. K. Lyszkowshi and D. Wallace, "Multiple fan having means for reducing beat frequency oscillations", United States Patent Publication, US 6,270,319 B1, (2001).

27. R. L. Clark, C. R. Fuller, "Optimal placement of piezoelectric actuators and polyvinylidene fluoride error sensors in active structural acoustic control approaches". J. *Acoust. Soc. Am.* **92** (3), pp. 1521-1533 (1992).

28. A. P. Berkhoff, "Optimum sensor-actuator distance for decentralized acoustic control". J. *Acoust. Soc. Am.* **110** (1) pp. 260-266, (2001).

29. S. Pulthasthan and R Pota. “The optimal placement of actuator and sensor for active noise control of sound-structure interaction systems”, *Smart Mater. Struct.* **17**(3) pp. 037001 (2008).

30. C. Duke, S. D. Sommerfeldt, K. L. Gee, C. V. Duke, “Optimization of control source locations in free-field active noise control using a genetic algorithm”, *Noise Control Eng.* **57** (3), (2009).

31. B. T. Wang, “Optimal placement of microphones and piezoelectric transducer actuators for far-field sound radiation control”, *J. Acoust. Soc. Am.*, **99**, pp. 2975–2984, (1996).

32. D. A. Manolas, I. Borchers and D. T. Tsahalis, “Simulataneous optimization of the sensor and actuator positions for an active noise and/or vibration control system using genetic algorithms,applied in a Donier aircraft”, *Eng. Comput.*, **17**, pp. 620–630, (2000)

33. Y. Guo, L. Zhang, L. L. Zhang, and J. X. Zhou, “Optimal placement of sensors for structural health monitoring using improved genetic algorithms.” *Smart Mater. Struct.* **13** 528 (2004).

34. S. Pottie and D. Botteldooren, “Optimal placement of secondary sources for active noise control using a genetic algorithm”, Proceedings of Inter-Noise 96, Liverpool, UK, Noise Control Foundation, Poughkeepsie, NY, pp. 1101–1104, (1996).

35. B. Monson, S. D. Sommerfeldt, K. L. Gee, “Improving compactness for active noise control of a small axial cooling fan”, *Noise Control Eng. J*, **55**, 397-407,(2007).

36. A. Gerard, A. Berry, M. Patrice, “Control of tonal noise from subsonic axial fan. Part 2:Active control simulations and experiments in free field”, *J. of Sound and vibration*, **288**, 1077-1104, (2005).

37. R. H. Thomas, R.A. Burdisso, C. R. Fuller, and W. F. O’Brien. “Active control of fan noise from a turbofan engine”. *AIAA J*. **32**, pp. 23-30, (1994).

38. B. T. Wang, “Optimal placement of microphones and piezoelectric transducer actuators for far-field sound radiation control”, *J. Acoust. Soc. Am.*, **99**, pp. 2975–2984, (1996).

39. P. A. Nelson and S. J. Elliot, Active Control of Sound, Academic, London, p. 436, (1992).

40. E Baugh, M Beltman, H Pokharna, “Cooling fan reduction apparatus, systems and methods”, US 73002744, Nov. 27,(2007).